

# Spectral Sparse Representation for Clustering: Evolved from PCA, K-means, Laplacian Eigenmap, and Ratio Cut

Zhenfang Hu<sup>\*</sup>, Gang Pan<sup>\*</sup>, Yueming Wang<sup>1</sup>, and Zhaohui Wu<sup>\*</sup>

<sup>\*</sup>College of Computer Science and Technology, Zhejiang University, China,  
fancij@zju.edu.cn, gpan@zju.edu.cn, wzh@zju.edu.cn

<sup>1</sup>Qiushi Academy for Advanced Studies, Zhejiang University, China,  
ymingwang@zju.edu.cn

May 22, 2017

## Abstract

Dimensionality reduction, cluster analysis, and sparse representation are basic components in machine learning. However, their relationships have not yet been fully investigated. In this paper, we find that the spectral graph theory underlies a series of these elementary methods and can unify them into a complete framework. The methods include PCA, K-means, Laplacian eigenmap (LE), ratio cut (Rcut), and a new sparse representation method developed by us, called spectral sparse representation (SSR). Further, extended relations to conventional over-complete sparse representations (e.g., method of optimal directions, KSVD), manifold learning (e.g., kernel PCA, multidimensional scaling, Isomap, locally linear embedding), and subspace clustering (e.g., sparse subspace clustering, low-rank representation) are incorporated. We show that, under an ideal condition from the spectral graph theory, PCA, K-means, LE, and Rcut are unified together. And when the condition is relaxed, the unification evolves to SSR, which lies in the intermediate between PCA/LE and K-mean/Rcut. An efficient algorithm, NSCrT, is developed to solve the sparse codes of SSR. SSR combines merits of both sides: its sparse codes reduce dimensionality of data meanwhile revealing cluster structure. For its inherent relation to cluster analysis, the codes of SSR can be directly used for clustering. Scut, a clustering approach derived from SSR reaches the state-of-the-art performance in the spectral clustering family. The one-shot solution obtained by Scut is comparable to the optimal result of K-means that are run many times. Experiments on various data sets demonstrate the properties and strengths of SSR, NSCrT, and Scut.

**Keywords:** sparse representation, spectral graph, dimensionality reduction, cluster analysis, PCA, K-means, spectral clustering, Laplacian eigenmap.

## 1 Introduction

As the rise of information age, we are overwhelmed by a large amount of data generated daily, e.g., images, videos, speeches, text, financial data, and biomedical data. But the information contained in these data is usually not explicit in their original forms. Data understanding becomes gradually urgent. In this paper, we focus on unsupervised learning, which tries to find hidden structure in unlabeled data. The intrinsic structure of data is often explored by representing the data in another form. Typically used methods include dimensionality reduction, cluster analysis, and sparse representation, which are among the cornerstones of machine learning.

However, the relationships among these methods have not been fully explored. We believe that the basic parts of machine learning deserve extensive investigation. This paper devotes to an attempt in this direction.

### 1.1 Dimensionality Reduction and Cluster Analysis

Dimensionality reduction and cluster analysis are two of the most traditional unsupervised learning methods, having wide-spread applications.

**Dimensionality reduction.** It aims at representing data by low-dimensional codes. On the one hand, it saves storage, considering many data we encounter are of high dimensions whose intrinsic dimensions, however, are much lower. On the other hand, noise may be reduced and the structure of data becomes prominent. The codes will preserve the relation of data as much as possible, e.g., distance between data points. The widely applied methods include: principal component analysis (PCA) [37], multidimensional scaling (MDS) [16], kernel PCA [57], nonnegative matrix factorization (NMF) [39], Isomap [62], locally linear embedding (LLE) [53], Laplacian eigenmap (LE) [4], and locality preserving projections (LPP) [35].

**Cluster analysis.** It tries to partition the data into disjoint groups such that similar data points are assigned to the same group and dissimilar data points are separated into different groups. In this way, the cluster structure of data is revealed. Various methods have been proposed, for example, centroid-based K-means clustering [42] and its distribution-based version: clustering via Gaussian mixture models (GMM) [7], connectivity-based hierarchical clustering [34], density-based DBSCAN [29], and graph-based spectral clustering [64, 18] such as ratio cut (Rcut) [11], normalized cut (Ncut) [59, 73, 47].

The two kinds of methods appear distinct: dimensionality reduction is concerned with fidelity where the data relation should be preserved faithfully, while cluster analysis focuses on semantic where the classes of data should be made clear. However, in a broad sense, both of them can be seen as code-based data representation methods. For cluster analysis, each data point is represented by one cluster, and its codes are indicator vector consisting of zeros and a 1, the index of which indicates the cluster membership. The codes of dimensionality reduction are compact, due to low dimensionality and fidelity, while the codes of cluster analysis are sparse, due to only one nonzero.

The above methods, according to the form of input data they work with, can be categorized into two types. One works with original data, e.g., PCA and K-means. The other works with similarity matrix, which stores the pair-wise relations of data, e.g., LE and spectral clustering. We can call the second type kernel methods, since usually the similarity matrix is constructed by some kernel function [64, 58].

Among the various methods of dimensionality reduction and cluster analysis, PCA, K-means, LE, and spectral clustering are the representative ones. They are based on principled mathematical formulations and are effective in practice. In this paper, we focus on these four methods. They appear very different at first sight. Some of them are dimensionality reduction methods while the others are cluster analysis methods. Some of them work with original data while the others work with similarity matrix. In fact, they are closely related. Some pair-wise connections have been found in the literature, including LE and Ncut [4], PCA and K-means [20], spectral clustering and K-means [18]. However, the relations remain pair-wise, they are not yet rigorously integrated into a unified framework.

## 1.2 Sparse Representation (SR)

Sparse representation is a more recently developed code-based representation method, which represents data with a dictionary and sparse codes. In existing SRs, the dictionary is generally over-complete, i.e., the size of dictionary (number of words/atoms) is larger than the data dimension. The codes are called sparse for only a few nonzero entries exist or dominate.

In the past several years, the communities of signal processing, computer vision, and pattern recognition had witnessed the great success of various SRs [9, 25, 68, 54], e.g., compressed sensing theory [23, 10, 9], over-complete dictionary learning, including [49], method of optimal directions (MOD) [28], KSVD [2]. In pattern recognition, sparse codes are frequently used as features for classification, e.g., face recognition [69], image classification [71, 8, 14].

Almost all prevalent SRs are over-complete SRs (OSRs). Except the special application in compressed sensing, OSRs are not related to dimensionality reduction. On the other hand, comparing with the popular applications in classification, the applications in clustering are few, the most well-known one is sparse subspace clustering (SSC) [27], which deals with clusters lying in a union of subspaces.

## 1.3 Our Work

In this paper, we deepen and complete the relations among PCA, K-means, LE,<sup>1</sup> and Rcut, so that they are unified together. Then, a new SR is developed, called spectral sparse representation (SSR), which evolves from the

---

<sup>1</sup>The LE we refer to hereafter is slightly different from the original one [4]. The definition will be given in later section. We call the original LE to be normalized LE for a reason that will be clear later.

unification of the four methods, bearing inherent relations to dimensionality reduction and cluster analysis. The spectral graph theory underlies all the methods and integrates them into a framework.

The idea can be briefly described as follows. PCA, LE, K-means, and Rcut are written into forms working with the same matrix, the Laplacian matrix from the spectral graph theory. The low-dimensional codes of PCA and LE are the leading eigenvectors of this matrix. When an ideal graph condition is met, which implies perfectly separable clusters exist in the data, the indicator vectors of K-means and Rcut become the leading eigenvectors, thus PCA, K-means, LE, and Rcut are unified. When the condition is relaxed, the leading eigenvectors become noisy indicator vectors, which are sparse and still contain some cluster information of the data, the unification then evolves to SSR.

The first step to the unification is to establish the bilateral conversion between PCA and LE, and that between K-means and Rcut. In effect, we convert the objective of one method into the form of the other. It turns out that PCA and K-means are equivalently working with a similarity matrix built by the Gram matrix of data, i.e., linear kernel matrix. So they can be converted to the forms of kernel methods. Roughly speaking, PCA and K-means are linear LE and linear Rcut respectively. Conversely, the similarity matrix used by LE and Rcut can be converted to a Gram matrix of some virtual data. Thus the objectives of LE and Rcut can be written into the forms of PCA and K-means respectively. Our theory includes two versions: one works with the original data, called linear version; the other works with the similarity matrix, called kernel version.

The second step to the unification is to bridge the link between Rcut and LE under an ideal graph condition. This is done through spectral graph theory [13, 45, 44], as [4] did. The solution of LE is a set of eigenvectors corresponding to the zero eigenvalues, and that of Rcut is a set of indicator vectors corresponding to the best partition. Under the condition, the two sets of vectors span the same subspace, and they are equivalent in the sense of a rotation transform. In brief, the indicator vectors become the leading eigenvectors of LE, that is Rcut and LE are unified. Based on the results, the equivalence between PCA and K-means is automatically built. Therefore, the unification of PCA, K-means, LE, and Rcut is established.

The unification evolves to SSR when the ideal condition is relaxed, i.e., in a noisy case. In this case, the leading eigenvectors of PCA and LE span the same subspace as the noisy version of the indicator vectors. We call the noisy indicator vectors sparse codes, since the codes of each data point is usually dominated by one entry, and the “noise” indeed quantitatively reflects the overlapping status of the clusters. We develop an algorithm, called NSCrT, to find a rotation matrix, by which the eigenvectors turn into the noisy indicator vectors. Furthermore, as an application of SSR, a clustering algorithm, sparse cut (Scut), is developed, which determines the cluster membership of each data point by simply checking the maximal entry of its code vector.

SSR can establish extended relations to a series of methods, including 1) OSRs, e.g., [49], MOD, KSVD, 2) manifold learning, e.g., kernel PCA, MDS, Isomap, LLE, and 3) subspace clustering, e.g., SSC, low-rank representation (LRR) [40].

A diagram of the relations between PCA, linear SSR, OSR, and K-means is shown in Figure 1 (it will be discussed in details in Section 8.1). The codes of the methods change from compact to sparse, and then to extreme sparse, leading to clustering. The main framework of our work is shown in Figure 2.

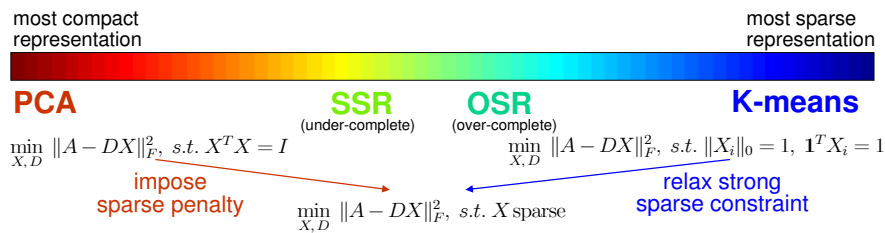


Figure 1: A diagram of the relations between dimensionality reduction, sparse representation, and cluster analysis, represented by PCA, linear SSR, OSR, and K-means.

The features and contributions of the paper are four-fold:

1. A spectral graph theory-based framework unifying dimensionality reduction, cluster analysis, and sparse representation has been established, including inherent relations between PCA, K-means, LE, Rcut, SSR, and extended relations to OSRs ([49], MOD, KSVD), manifold learning (kernel PCA, MDS, Isomap, LLE), and subspace clustering (SSC, LRR).

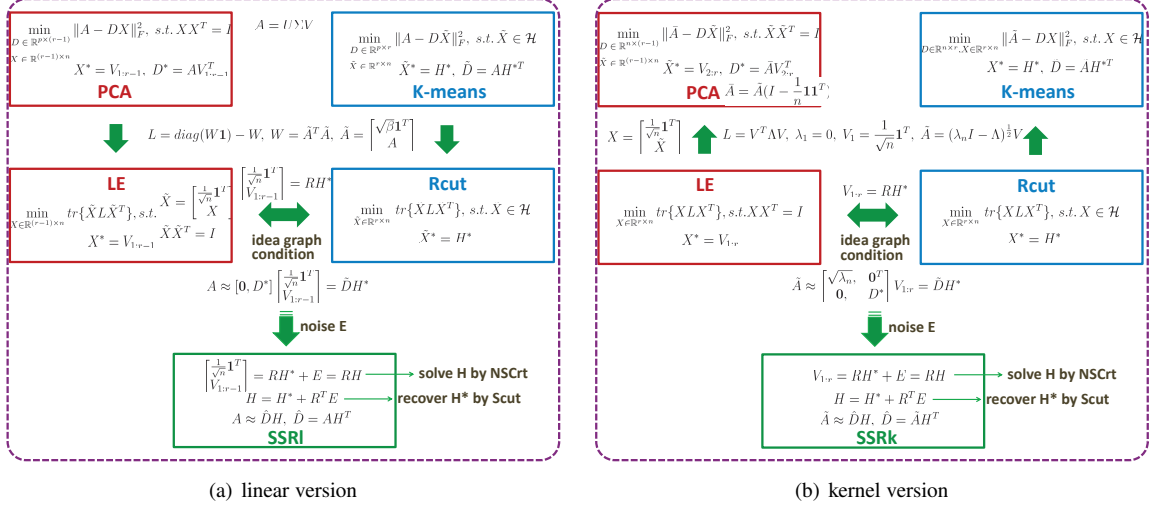


Figure 2: Main framework of the paper.

2. A new sparse representation, SSR, is developed. It is inherently related to dimensionality reduction and cluster analysis, and shares broad relations to many other methods. Lying in the intermediate between dimensionality reduction and cluster analysis, SSR combines merits of both sides. It achieves dimensionality reduction with the same fidelity as PCA/LE meanwhile revealing cluster structure of data. In contrast to the hard clustering nature of K-means/Rcut, SSR is soft and descriptive: it reveals the underlying clusters, and also describes the overlapping status of them. In contrast to OSRs, the sparse codes of SSR can be directly used for clustering, and the sparsity in SSR is implicitly determined by the data structure rather than imposed explicitly. If the clusters overlap less, the codes become sparser, and vice versa. Finally, SSR has two versions, a linear version, which is under-complete, complementing to OSRs, and a more powerful kernel version. For both versions, sparse codes of new data that are out of the sample set can be easily obtained.
3. An algorithm, NSCrt, is developed to solve the sparse codes of SSR. It is simple yet efficient, having a linear computational complexity about the data size. Experimental results demonstrated that, it can effectively recover the underlying solutions.
4. A clustering algorithm, Scut, is derived from SSR, which performs clustering by checking the maximal entry of each sparse code-vector. Owing to the good performance of NSCrt, Scut outperforms K-means based spectral clustering methods, which depend on initialization and easily get trapped in local minima. The one-shot solution obtained by Scut is comparable to the optimal result of K-means that are run many times.

The rest of the paper is arranged as follows. Section 2 introduces the related work. Section 3 reviews PCA, K-means, Rcut, and LE, and introduces the most appropriate forms for the unification. Section 4 establishes the bilateral conversions between PCA and LE, K-means and Rcut. Section 5 presents the equivalence relation of LE and Rcut, and unifies the four methods. Section 6 proposes SSR, out-of-sample extensions, NSCrt, and Scut. Section 7 shows the experimental results. Section 8 investigates the extended relations to other methods. The paper is concluded with Section 9.

**Notations.** The major notations used are listed in Table 1.

## 2 Related Work

First of all, we should clarify that the unifying framework we investigate is different to many frameworks or unified views in the literature, e.g., [6, 70, 17], which usually focus on studying the general objective function shared by a set of methods, whose contents as well as solutions may be unrelated to each other. Our framework investigates

Table 1: Notations.

Notation	Interpretation
$\mathbf{1}$	A vector of uniform value 1.
$\text{null}(A)$	Null space of matrix $A$ .
$\text{span}(A)$	Subspace spanned by columns (or rows, when clear under the context) of $A$ .
$\text{diag}(v)$	A diagonal matrix with the diagonal being vector $v$ .
$A = [A_1, \dots, A_n] \in \mathbb{R}^{p \times n}$	Data matrix with $n$ samples of dimension $p$ arranged column-wise.
$F \in \mathbb{R}^{K \times n}$	Indicator vectors/matrix. The $k$ th row $F_k$ is the indicator vector of the $k$ th cluster $C_k$ : $F_{ki} = 1$ if $A_i \in C_k$ , and $F_{ki} = 0$ otherwise. $F_i$ denote the $i$ th column of $F$ . Note that $FF^T = \text{diag}([n_1, \dots, n_K])$ , i.e., $F_{k_1} F_{k_2}^T = n_k$ , where $n_k$ is the size of $C_k$ , if $k_1 = k_2$ ; and $F_{k_1} F_{k_2}^T = 0$ otherwise.
$\mathcal{F} = \{F \in \mathbb{R}^{K \times n} \mid \ F_i\ _0 = 1, \mathbf{1}^T F_i = 1, \forall i\}$	All possible $K$ -partitions of $n$ samples.
$H^* \in \mathbb{R}^{K \times n}$	Normalized indicator vectors/matrix. $H^* = (FF^T)^{-1/2} F$ . It implies $H_k^* = \frac{1}{\sqrt{n_k}} F_k$ , $\ H_k^*\ _2 = 1$ , and $H^* H^{*T} = I$ . In SSR, we use $H$ to denote the noisy version of $H^*$ , i.e., sparse codes.
$\mathcal{H} = \{H^* \mid H^* = (FF^T)^{-1/2} F, F \in \mathcal{F}\}$	Normalized version of $\mathcal{F}$ .
$V_{1:r}$	The leading $r$ eigenvectors if $V$ is an eigenvector matrix.

the inherent relations, e.g., the equivalences of solutions and the conditions when they hold. Besides, although there are combined applications of dimensionality reduction, cluster analysis, and SR, we do not consider heuristic hybrid models, e.g., different methods are added together or form a pipeline to accomplish certain task. We will introduce the related work below: pair-wise relations of PCA, K-means, LE, and spectral clustering; OSRs; and clustering methods close to Scut.

## 2.1 Pair-wise Relations of PCA, K-means, LE, and Spectral Clustering

**Normalized LE and Ncut** [4]: their objectives can be written into similar forms except that spectral clustering additionally requires the variable to be an indicator matrix for the purpose of clustering. The solution of normalized LE is a set of generalized eigenvectors, while that of Ncut is indicator vectors. When a condition is met, which is in fact the ideal graph condition in this paper, the indicator vectors become the leading generalized eigenvectors, so the two methods become equivalent. When the condition is nearly met, the generalized eigenvectors are a rotation of some noisy indicator vectors. Thus, clustering is usually done by postprocessing the generalized eigenvectors, e.g., applying K-means on the generalized eigenvectors. In addition to Normalized LE and Ncut, there is a more elementary counterpart, LE and Rcut, which will make the connections to PCA and K-means straightforward. However, they have been largely overlooked. In this paper, we will focus on LE and Rcut.

**PCA and K-means** [20]: their objectives can be written into similar forms except that PCA drops a constant component and K-means constrains a variable to be discrete indicator. PCA is thus viewed as a relaxation of K-means. The relaxation relation indicates that clustering may be done by applying K-means on the normalized principal components of PCA, i.e., some leading eigenvectors. It is easy to see that this pair shares many common features with the first pair. But this analogy may be ignored. In this paper, we will convert PCA and K-means to LE and Rcut respectively, and then with the help of spectral graph theory, it is discovered that PCA and K-means are inherently related, beyond sharing similar forms. They are even exactly equivalent under an ideal graph condition. It further reveals that the heuristic clustering scheme of applying K-means on the normalized PCs is in fact a linear Rcut algorithm. Similar clustering strategies that apply dimensionality reduction as preprocessing have been studied [15] and frequently applied, however, the preprocessing is mostly considered for the reasons of efficiency, denoising, etc. rather than inherent relation.

**Spectral clustering and kernel K-means** [18]: the trace minimization or maximization form of spectral clustering can be converted to the trace maximization form of (weighted) kernel K-means, so spectral clustering can be solved by (weighted) kernel K-means. However, on the one hand, the conversion stops at kernel K-means and does not go further to the dictionary-based representation. In this paper, we will show that the dictionary form can enrich our understanding of spectral clustering. On the other hand, the conversion from K-means to spectral clustering is absent.<sup>2</sup> We will supplement this part and show that this conversion will lead to a linkage between dimensionality reduction and cluster analysis.

<sup>2</sup>Among the spectral clustering, Ncut corresponds to weighted K-means, while Rcut corresponds to K-means. The conversion from K-means to Rcut is feasible. However, in the same rigorous sense, the conversion from weighted K-means to Ncut seems infeasible. Hence, we focus on K-means and Rcut in this paper.

The above relations remain pair-wise and have not yet been integrated into a unified framework.

## 2.2 Over-complete Sparse Representation (OSR)

The representative work of OSRs include compressed sensing theory, sparse and redundant dictionary learning and their applications in pattern recognition.

Compressed sensing theory [23, 10, 9] states that if a signal is sparse under some basis, then far fewer measurements than Shannon theorem indicates are required to reconstruct the signal. Over-complete dictionary is designed and should satisfy good mutual coherence property, i.e., atoms of the dictionary are not close to each other. If the signal is intrinsically sparse enough, the sparse codes are guaranteed to be solved exactly by an  $\ell_0$ -norm based greedy algorithm, orthogonal matching pursuit (OMP) [50], or by an  $\ell_1$ -norm based convex optimization, basis pursuit (BP) [12]. In this case, the signal can be exactly reconstructed. The compressed sensing theory is concerned with signal compression and reconstruction, in this paper, we will focus on the semantic aspect, i.e., cluster structure.

[49], MOD [28], and KSVD [2] learn an over-complete dictionary and sparse codes, based on different sparsity penalties and optimizations. Taking advantage of the reconstruction power of SR, KSVD has achieved good performance on a series of image processing problems [25], e.g., image compression, denoising, deblurring, inpainting, and super resolution. The model and optimization process of KSVD are generalized from those of K-means [2]. However, effective application of KSVD in clustering is hardly found.

In pattern recognition, after OSRs are solved, the sparse codes are frequently used as features for classification, e.g., face recognition [69], image classification [71, 8, 14]. [31] developed a kernel SR extending the work of [69] and [71]. The kernel trick is applied on the dictionary rather than the data. Since the dictionary is unknown beforehand, the optimization is complex. On the other hand, there are few work on clustering. Except in model combination way, e.g., [51, 22], the most famous one may be sparse subspace clustering (SSC) [27], which deals with data that lie in a union of independent low-dimensional linear/affine subspaces, with each subspace corresponding to a cluster.

In summary, OSRs are mainly applied to signal compression, image representation, and image classification. They are not related to cluster analysis and dimensionality reduction. The applications in clustering are few.

## 2.3 Spectral Clustering Methods

Spectral clustering usually consists of two steps: first some eigenvectors are solved, then some post-processing techniques are employed to recover the discrete indicator vectors from the eigenvectors, i.e., finishing clustering. Scut follows this manner. Besides the most simple post-processing technique, K-means, as classical spectral clusterings used [64], there are some other efforts have been made.

[75] is the closest to Scut. It tried to find a rotation matrix through which rows of the eigenvectors (column-wise) best align with the canonical coordinate system. Then as Scut, non-maximum suppression was applied to finish clustering. However, the rotation matrix is solved by gradient descent under some objective, whose computational cost is high when the number of clusters becomes somewhat large. [73] directly found a set of discrete indicator vectors and a rotation matrix such that the discrete indicator vectors approximate the row-normalized eigenvectors after the rotation. Rather than finding a rotation matrix, [74] found a set of soft indicator vectors by nonnegative factorization of a transformed similarity matrix, then non-maximum suppression was applied.

The post-processing step is important for spectral clustering. Although many recent variants of spectral clustering were proposed, producing various relaxed indicator matrices, e.g., [65, 48, 72], they still rely on the above techniques, especially K-means, to finish the clustering. Little progress was observed in dealing with the post-processing.

## 3 Reviews: PCA, K-means, Rcut, and LE

The section will introduce the classical formulations of PCA, K-means, Rcut, and LE, as well as the most appropriate forms for the unification: the dictionary representation forms for PCA and K-means, the trace optimization forms for Rcut and LE. Along with them, important properties and interpretations are elaborated.

### 3.1 Principal Component Analysis (PCA)

Given mean-removed data matrix  $A \in \mathbb{R}^{p \times n}$  ( $A\mathbf{1} = \mathbf{0}$ ), PCA [37] approximates the data by representing them in another basis, called loadings  $Q = [Q_1, \dots, Q_r] \in \mathbb{R}^{p \times r}$  ( $r \ll p$ ):  $A_i \approx QY_i, \forall i$ , where  $Y_i \in \mathbb{R}^r$  are the low-dimensional codes, called principal components (PCs). The loadings are computed sequentially by maximizing the scaled covariance matrix  $C = AA^T$ :

$$\max_{Q_i} Q_i^T C Q_i, \text{ s. t. } \|Q_i\|_2 = 1, Q_i^T Q_j = 0, j = 1, \dots, i-1. \quad (1)$$

Let  $A = U\Sigma V$  be the compact SVD of  $A$ ,<sup>3</sup> where  $\Sigma \in \mathbb{R}^{m \times m}$ , and  $m$  is the rank of  $A$ . Then  $C = U\Sigma^2 U^T$ , and the solution is  $Q^* = U_{1:r}, Y^* = Q^{*T} A = \Sigma_{1:r} V_{1:r}$ , where  $\Sigma_{1:r}$  is a diagonal matrix containing the first  $r$  singular values.

PCA can also be derived from the well-known Eckart-Young theorem [24], where it takes a dictionary representation form:

**Theorem 1. (Eckart-Young Theorem)** Let  $A = U\Sigma V$  be the compact SVD of  $A$ . A particular solution of the rank  $r$  ( $r \leq \text{rank}(A)$ ) approximation of  $A$

$$\min_{D, X} \|A - DX\|_F^2, \text{ s. t. } XX^T = I, \quad (2)$$

where  $D \in \mathbb{R}^{p \times r}$  and  $X \in \mathbb{R}^{r \times n}$ , is provided by

$$X^* = V_{1:r}, D^* = AX^{*T} = U_{1:r}\Sigma_{1:r}. \quad (3)$$

In fact, for any rotation matrix  $R \in \mathbb{R}^{r \times r}$ ,  $R^T R = I$ ,  $RX^*$  and  $D^* R^T$  also constitutes a solution.  $V_{1:r}$  are the normalized PCs, where the weights  $\Sigma_{1:r}$  have been transferred to the loadings, and  $U_{1:r}\Sigma_{1:r}$  becomes the scaled loadings. If normality were imposed on  $D$  rather than  $X$ , PCA could be exactly recovered.

In this paper, we take (2) as the formulation of PCA. It has the following interpretations: 1) each sample is approximated by a dictionary representation, e.g.,  $A_i \approx DX_i$ , namely a linear combination of the atoms (columns) of dictionary  $D$  with the codes  $X_i$ . 2) The dictionary in turn comes from the linear combinations of the samples with transpose of the codes,  $D^* = AX^{*T}$ . 3) Eliminating the dictionary, we have  $A_i \approx A(X^{*T} X_i^*)$ , i.e.,  $A_i$  can be approximated by a linear combination of the whole data set with weight vector  $X^{*T} X_i^*$ . The Gram matrix of codes,  $X^{*T} X^*$ , encodes a linear relationship of the data within rank- $r$  limitation.

### 3.2 K-means

Given data matrix  $A \in \mathbb{R}^{p \times n}$ , K-means [42, 20] aims to partition the data into  $K$  clusters via minimizing the within-cluster variance:

$$\min_{C_1, \dots, C_K, D} \sum_{k=1}^K \sum_{A_i \in C_k} \|A_i - D_k\|_2^2, \quad (4)$$

where  $C_k$  is the  $k$ th cluster,  $D = [D_1, \dots, D_K] \in \mathbb{R}^{p \times K}$  are the  $K$  cluster centers. After initializing  $D$ , K-means finds a locally optimal solution via alternating two steps: given  $D$ , assign each sample to the nearest cluster center; given the current partition, update  $D_k$  by the mean of its members.

Using indicator matrix, the above objective can be written in a dictionary representation form [20]:

$$\min_{D, F} \sum_{i=1}^n \|A_i - DF_i\|_2^2 = \|A - DF\|_F^2, \text{ s. t. } F \in \mathcal{F}. \quad (5)$$

It can be solved alternately. Given  $D$ , solving  $F_i$  corresponds to the nearest-center search; given  $F$ , it becomes a linear regression problem, and  $D^* = AF^\dagger = AF^T (FF^T)^{-1}$ . Since  $FF^T$  is a diagonal matrix of the cluster sizes, the atoms of  $D^*$  are the averages of cluster members. Hence, the solution process is exactly identical to that of traditional K-means.

<sup>3</sup>By default we use the compact form of SVD in this paper, and assume a descending order of the singular values.

Substituting  $D^* = AF^T(FF^T)^{-1}$  into (5), we obtain  $\min_F \|A - AF^T(FF^T)^{-1}F\|_F^2$ , s. t.  $F \in \mathcal{F}$ . Using the normalized indicator instead, it is equivalent to

$$\min_X \|A - AX^T X\|_F^2, \text{ s. t. } X \in \mathcal{H}, \quad (6)$$

and

$$\min_{D, X} \|A - DX\|_F^2, \text{ s. t. } X \in \mathcal{H}, \quad (7)$$

with  $D^* = AX^{*T}$ .<sup>4</sup>

In this paper, we take (7) as the formulation of K-means. It has the following interpretations: 1) Each sample is allowed to be represented by only one atom,  $A_i \approx DX_i$ ,  $\|X_i\|_0 = 1$ . The representation error is thus large. 2) Each atom is a weighted average of the cluster members,  $D_k^* = AX_k^{*T}$ . But note that it is not a proper cluster center now, since  $X_k$  does not sum to 1. 3) Eliminating the dictionary, we get  $A_i \approx A(X^{*T} X_i^*)$ . The weight vector  $X^{*T} X_i^*$  takes the form of, e.g.,  $[\frac{1}{n_k}, \dots, \frac{1}{n_k}, 0, \dots, 0]^T$ , and they always sum to 1,  $\mathbf{1}^T(X^{*T} X_i^*) = 1$ . It implies that  $A_i$  is approximated by the mean of the cluster members, i.e., cluster center. The Gram matrix of the codes  $X^{*T} X^*$  reflects the cluster structure of the data.

### 3.3 Ratio Cut (Rcut)

Given an undirected graph of  $n$  vertices (data points), with the adjacency matrix defined to be a similarity matrix  $W \in \mathbb{R}^{n \times n}$ , measuring the pairwise similarities between data points,  $W_{ij} = W_{ji} \geq 0$ , Rcut [11, 64] seeks a partition via minimizing the one-versus-rest weights:

$$\min_{C_1, \dots, C_K} \sum_{k=1}^K \frac{g(C_k, \bar{C}_k)}{n_k}, \quad (8)$$

where  $C_k$  is the  $k$ th cluster, and  $\bar{C}_k$  is the complement of it,  $g(C_k, \bar{C}_k) = \sum_{i \in C_k} \sum_{j \in \bar{C}_k} W_{ij}$ ,  $n_k$  is the size of  $C_k$ .

The objective can be expressed more explicitly by the indicator notation together with the graph Laplacian matrix [64]:

$$\min_{C_1, \dots, C_K} \sum_{k=1}^K \frac{g(C_k, \bar{C}_k)}{n_k} \quad (9)$$

$$= \min_F \sum_{k=1}^K \frac{F_k L F_k^T}{F_k F_k^T}, \text{ s. t. } F \in \mathcal{F} \quad (10)$$

$$= \min_X \sum_{k=1}^K X_k L X_k^T, \text{ s. t. } X_k = (F_k F_k^T)^{-1/2} F_k \quad (11)$$

$$= \min_X \text{tr}\{X L X^T\}, \text{ s. t. } X \in \mathcal{H}. \quad (12)$$

$L$  is the Laplacian matrix defined as  $L = S - W$ , where  $S$  is a diagonal degree matrix with the  $i$ th diagonal element being the sum of weights on the  $i$ th row,  $s_i = \sum_{j=1}^n W_{ij}$ . In the above objectives, the equivalence of (9) and (10) as well as the solution of (12) depend on some properties of the Laplacian matrix [45, 44] and the ideal graph condition. These properties and the condition are fundamental to the unification and SSR. We now introduce.

Firstly, there is an elementary property of Laplacian matrix:

$$\forall f \in \mathbb{R}^n, f^T L f = \sum_{i < j} (f_i - f_j)^2 W_{ij} \geq 0. \quad (13)$$

Based on this elementary property, the following properties can be derived:

1.  $L$  is positive semi-definite.

<sup>4</sup>For simplicity, we will frequently use the symbol  $D$  to represent dictionaries in this paper. However, they may not be the same variable when appearing in different objectives, e.g., (5) and (7).



2. When  $f$  is an indicator vector for  $C_k$ ,  $f^T L f = g(C_k, \bar{C}_k)$ .
3.  $\text{null}(L) \neq \{0\}$ . Vector  $\mathbf{1} \in \mathbb{R}^n$  is always an eigenvector of eigenvalue 0.
4. The multiplicity of eigenvalue 0 equals the number of connected components of the graph, and the  $K$  indicator vectors of the partition span the eigenspace of eigenvalue 0.

The equivalence of (9) and (10) is due to property 2. Property 4 plays a key role in the unification, and it is closely related to the ideal graph condition. The condition was informally called “ideal case” in the literature [64, 47]. We define it precisely:

**Definition 2. (Ideal graph condition)** Targeting for  $K$  clusters, if there are exactly  $K$  connected components in the graph, then the graph (or similarity matrix) is called ideal (with respect to  $K$  clusters).

The condition implies the between-cluster weights are all zero:  $W_{ij} = 0$ , if the  $i$ th and  $j$ th points are of different clusters. If members in the same cluster are arranged consecutively, the similarity matrix would consist of  $K$  diagonal blocks, and there are no sub diagonal blocks in each block.

However, the condition is often met *nearly* in practice: some nonzero weights exist between clusters. If arranged orderly, the similarity matrix would consist of  $K$  noisy diagonal blocks. Furthermore, according to matrix perturbation theory [21, 64]: 1) the  $K$  smallest eigenvalues are close to 0, with the smallest one still being 0; 2) the eigenspace is spanned by the  $K$  noisy indicator vectors, which do not deviate much from those in the ideal case; 3) the  $K$  eigenvectors, noted by  $V \in \mathbb{R}^{K \times n}$ , are a rotation of the  $K$  noisy indicator vectors  $H$ , i.e.,  $V = RH$ , where  $R$  is a unitary matrix.

Based on the above properties, we now introduce the solution scheme of Rcut. Objective (12) is hard to solve due to the discrete nature of  $X$ . For this reason, it is relaxed to

$$\min_X \text{tr}\{X L X^T\}, \text{ s. t. } X X^T = I, \quad (14)$$

where the discrete constraint is ignored. By the Ky Fan theorem [30], the solution set consists of all the rotations of the  $K$  smallest eigenvectors of  $L$ . Traditionally, the clustering is finished by applying K-means on the columns of these eigenvectors. The underlying rationale, which inspires SSR and Scut, is explained below.

When the graph is ideal, the underlying indicator matrix  $H^*$  would be the smallest eigenvectors, thus it constitutes a solution. Note that the  $i$ th column of  $H^*$ ,  $H_i^* \in \mathbb{R}^K$ , is the indicator vector of the  $i$ th data point: there is only one nonzero entry, and the index of it signals the cluster membership. All members of a cluster share the same pattern, and the indicator vectors of two data points belonging to different clusters are orthogonal. However, in numerical computation, the computed eigenvectors may be a rotated version,  $V = RH^*$ . The indicator structure disappears. Nevertheless, members of a cluster still share the same column pattern, and orthogonality is preserved. K-means can be applied on these columns to finish clustering. When the graph is nearly ideal, the eigenvectors are rotated noisy indicators. In this case, to finish clustering, some post-processing technique, e.g., K-means, is more necessary.

### 3.4 Laplacian Eigenmap (LE)

LE [4] is a dimensionality reduction algorithm that works with the same similarity matrix  $W$  as Rcut. It finds low-dimensional codes  $X_i \in \mathbb{R}^r$  for the  $i$ th data:

$$\min_X \frac{1}{2} \sum_{i,j} \|X_i - X_j\|_2^2 W_{ij} = \text{tr}\{X L X^T\}, \text{ s. t. } X X^T = I, \quad (15)$$

where  $X_i$  is the  $i$ th column of  $X$ ,  $L = S - W$  is the Laplacian matrix of  $W$ . The constraint  $X X^T = I$  is to avoid trivial solution.<sup>5</sup> The left-hand side of (15) implies that if a data pair is close ( $W_{ij}$  being large), their codes should be close too ( $\|X_i - X_j\|_2^2$  being small). In this way, the data relationship contained by  $W$  is approximately preserved by the codes. The equivalence of the left-hand side and the right-hand side is due to property (13) of the Laplacian matrix.<sup>6</sup>

<sup>5</sup>The original LE imposes  $X S X^T = I$ , whose counterpart in spectral clustering is Ncut [59, 4]. However, the simplified version here, whose counterpart in spectral clustering is Rcut, is more elementary, and it makes the connections to PCA and K-means feasible.

<sup>6</sup>Note that the right-hand side takes exactly the form of the relaxed Rcut (14). However, the task here focuses on representation rather than clustering. It does not care whether the data has cluster structure or not.

According to the right hand side of (15), any rotation of the  $r$  smallest eigenvectors of  $L$  is a qualified solution. Let  $L = V^T \Lambda V$  be the full spectral decomposition of  $L$ ,<sup>7</sup> where  $V_1 = \frac{1}{\sqrt{n}} \mathbf{1}^T$  is the smallest eigenvector (see property 1 and 3 of the Laplacian matrix). For the purpose of dimensionality reduction, the constant component  $V_1$  is often omitted. We can either restrict  $X\mathbf{1} = \mathbf{0}$  to obtain  $r$  dimensional codes  $X^* = V_{2:r+1}$ , or restrict  $X = \begin{bmatrix} \frac{1}{\sqrt{n}} \mathbf{1}^T \\ \tilde{X} \end{bmatrix}$  to obtain  $r - 1$  dimensional codes  $\tilde{X}^* = V_{2:r}$ . In this paper, we adopt the latter scheme, and sometimes also use (15).

## 4 Bilateral Conversions: PCA $\leftrightarrow$ LE, K-means $\leftrightarrow$ Rcut

We begin the unification by establishing the bilateral conversions between PCA and LE, K-means and Rcut. We will convert the objective of one method into the form of the other. It will turn out that PCA and K-means are equivalently working on a similarity matrix defined by the Gram matrix of data. Consequently, they can be converted to the forms of kernel methods. Briefly, PCA and K-means are linear cases of LE and Rcut respectively. Conversely, the similarity matrix used by LE and Rcut can be converted to a Gram matrix of some virtual data, enabling the objectives of them to be written into the forms of PCA and K-means respectively.

### 4.1 PCA $\rightarrow$ LE

For consistency, we assume PCA is to find  $r - 1$  PCs hereafter.

**Proposition 3.** (PCA  $\rightarrow$  LE) PCA is a special LE that uses linear kernel. The objective of PCA

$$\min_{D, X} \|A - DX\|_F^2, \text{ s. t. } XX^T = I, \quad (16)$$

where  $A\mathbf{1} = \mathbf{0}$ ,  $X \in \mathbb{R}^{(r-1) \times n}$ ,  $r - 1 \leq \text{rank}(A)$ , can be converted to the form of LE

$$\min_X \text{tr}\{\tilde{X}L\tilde{X}^T\}, \text{ s. t. } \tilde{X} = \begin{bmatrix} \frac{1}{\sqrt{n}} \mathbf{1}^T \\ X \end{bmatrix}, \tilde{X}\tilde{X}^T = I. \quad (17)$$

$L$  is the Laplacian matrix of  $W$ , and  $W = \tilde{A}^T \tilde{A}$ , where  $\tilde{A} = \begin{bmatrix} \sqrt{\beta} \mathbf{1}^T \\ A \end{bmatrix}$  is called augmented data, and  $\beta = -\min_{ij} (A^T A)_{ij}$  so that  $W_{ij} \geq 0$ ,  $\forall i, j$ .  $W$  is a kernel matrix built by the linear kernel function  $\phi(A_i, A_j) = A_i^T A_j + \beta$ .

*Proof.* In the following, we will eliminate the dictionary of PCA and convert PCA to the trace form, after that we define a similarity matrix to be the Gram matrix of data, and then apply a padding trick to make it nonnegative, finally we convert it to the Laplacian form.

We now go into details. Substituting  $D = AX^T$  into (16), we obtain  $\min_X \|A - AX^T X\|_F^2$ , s. t.  $XX^T = I$ . Since  $XX^T = I$ ,  $X^T X$  is a projection matrix, then by the Pythagorean theorem,

$$\|A - AX^T X\|_F^2 = \|A\|_F^2 - \|AX^T X\|_F^2 = \text{tr}\{A^T A\} - \text{tr}\{X A^T A X^T\}. \quad (18)$$

Hence the objective is equivalent to  $\min_X \text{tr}\{X(-A^T A)X^T\}$ , s. t.  $XX^T = I$ . In this form, PCA is close to LE. Define the similarity matrix to be  $W = A^T A$ , which is in fact built by linear kernel. By  $A\mathbf{1} = \mathbf{0}$ ,  $S = \text{diag}(W\mathbf{1}) = \mathbf{0}$ , so  $(-A^T A)$  is a Laplacian matrix, except that  $W$  may not be nonnegative. Again, by  $A\mathbf{1} = \mathbf{0}$ ,  $\mathbf{1}$  is a singular vector of  $A$  with singular value 0. Then according to the Eckart-Young theorem,  $X^*$  must be orthogonal to  $\mathbf{1}$ , so we can restrict  $X\mathbf{1} = \mathbf{0}$ , and the objective is equivalent to

$$\begin{aligned} & \min_X -\text{tr}\{X(\beta \mathbf{1}\mathbf{1}^T + A^T A)X^T\} - \left(\frac{1}{\sqrt{n}} \mathbf{1}\right)^T (\beta \mathbf{1}\mathbf{1}^T + A^T A) \left(\frac{1}{\sqrt{n}} \mathbf{1}\right), \text{ s. t. } \begin{cases} X^T X = I \\ X\mathbf{1} = \mathbf{0} \end{cases} \\ & = \min_X \text{tr}\{\tilde{X}(-\tilde{A}^T \tilde{A})\tilde{X}^T\}, \text{ s. t. } \tilde{X} = \begin{bmatrix} \frac{1}{\sqrt{n}} \mathbf{1}^T \\ X \end{bmatrix}, \tilde{X}\tilde{X}^T = I. \end{aligned} \quad (19)$$

<sup>7</sup>By default we use the full form of spectral decomposition for the Laplacian matrix in this paper, which includes all zero eigenvalues, and we assume an ascending order of the eigenvalues.

In above, firstly we padded  $A^T A$  uniformly with  $\beta \geq 0$  to make  $A^T A$  nonnegative, e.g., choosing  $\beta = -\min_{ij} (A^T A)_{ij}$  (Since  $A\mathbf{1} = \mathbf{0}$ , surely  $\min_{ij} (A^T A)_{ij} \leq 0$ ); secondly we augmented  $X$  to be  $\tilde{X}$ . The padding trick can be interpreted as translating  $A$  along a new dimension so that the inner products of all data-pairs become nonnegative.

Finally, since  $S = \text{diag}(\tilde{A}^T \tilde{A}\mathbf{1}) = \beta n I$  and  $\tilde{X}\tilde{X}^T = I$ , we can turn (19) into a problem with respect to the Laplacian matrix  $L = \beta n I - \tilde{A}^T \tilde{A}$ , which is (17), a LE that uses linear kernel.  $\square$

By the equivalence of the objectives, we can obviously obtain the equivalence of the solutions.

**Corollary 4.** *The solutions of  $X$  in (16) and (17) are equivalent. Let the SVD of  $A$  be  $A = U\Sigma V$ , one common solution is  $X^* = V_{1:r-1}$ .*

During the conversions, the right singular vectors of  $A$  are preserved. It can be shown that

$$\tilde{A} = \tilde{U}\tilde{\Sigma}\tilde{V} = \begin{bmatrix} 1 & \\ & U \end{bmatrix} \begin{bmatrix} \sqrt{\beta n} & \\ & \Sigma \end{bmatrix} \begin{bmatrix} \frac{1}{\sqrt{n}}\mathbf{1}^T \\ V \end{bmatrix}, \quad (20)$$

i.e., the SVD of  $\tilde{A}$  is also an augmentation of that of  $A$ . Further, we obtain the spectral decomposition of  $L$ :

$$\begin{aligned} L = \beta n I - \tilde{A}^T \tilde{A} &= \begin{bmatrix} \tilde{V}^T & \hat{V}^T \end{bmatrix} \begin{bmatrix} \beta n I - \tilde{\Sigma}^2 & \\ & \beta n I \end{bmatrix} \begin{bmatrix} \tilde{V} \\ \hat{V} \end{bmatrix} \\ &= \begin{bmatrix} \frac{1}{\sqrt{n}}\mathbf{1} & V^T & \hat{V}^T \end{bmatrix} \begin{bmatrix} 0 & & \\ & \beta n I - \Sigma^2 & \\ & & \beta n I \end{bmatrix} \begin{bmatrix} \frac{1}{\sqrt{n}}\mathbf{1}^T \\ V \\ \hat{V} \end{bmatrix}, \end{aligned} \quad (21)$$

where  $\hat{V}$  is the complement of  $\tilde{V}$ , i.e.,  $[\tilde{V}^T, \hat{V}^T]$  forms a unitary matrix. By (21), one solution of LE is  $X^* = V_{1:r-1}$ , equivalent to that of PCA.

## 4.2 K-means $\rightarrow$ Rcut

**Proposition 5. (K-means  $\rightarrow$  Rcut)** *Concerning objectives, K-means is a special Rcut that uses linear kernel. The objective of K-means*

$$\min_{D, X} \|A - DX\|_F^2, \text{ s. t. } X \in \mathcal{H}, \quad (22)$$

where  $X \in \mathbb{R}^{K \times n}$ , can be converted to the form of Rcut

$$\min_X \text{tr}\{X L X^T\}, \text{ s. t. } X \in \mathcal{H}, \quad (23)$$

where  $L$  is a Laplacian matrix defined as Proposition 3.

*Proof.* It follows most of the steps of Proposition 3. Since  $X X^T = I$ ,  $X^T X$  is a projection matrix, by (18), (6) is equivalent to  $\max_X \text{tr}\{X A^T A X^T\}$ , s. t.  $X \in \mathcal{H}$ . Applying the padding trick, and since  $\text{tr}\{X \mathbf{1} \mathbf{1}^T X^T\} = n$ , it is equivalent to

$$\min_X \text{tr}\{X(\beta n I - (\beta \mathbf{1} \mathbf{1}^T + A^T A))X^T\}, \text{ s. t. } X \in \mathcal{H} = \min_X \text{tr}\{X L X^T\}, \text{ s. t. } X \in \mathcal{H}, \quad (24)$$

where  $\beta = -\min_{ij} (A^T A)_{ij}$ . This is exactly the form of Rcut that uses linear kernel.  $\square$

**Corollary 6.** *The solutions of  $X$  in (22) and (23) are equivalent, whereas the algorithmic results of applying K-means to (22) and applying Rcut to (23) may be different. Let  $A = U\Sigma V$  be the SVD of  $A$ , where  $\Sigma \in \mathbb{R}^{m \times m}$ . Assume  $K \leq m + 1$ . In (22), K-means algorithm equivalently works with the full PCs  $\Sigma V$ . In (23), Rcut algorithm applies K-means algorithm on the leading  $K - 1$  normalized PCs  $V_{1:K-1}$ .*

*Proof.* Since K-means is rotation-invariant, working with  $U\Sigma V$  is equivalent to working with  $\Sigma V$  for K-means. On the other hand, Rcut algorithm applies K-means on the smallest eigenvectors of  $L$ , which is  $[\frac{1}{\sqrt{n}}\mathbf{1}, V_{1:K-1}^T]^T$  by (21), and since K-means is translation-invariant too, it is equivalent to applying K-means on  $V_{1:K-1}$ , i.e., the first  $K - 1$  PCs with singular values ignored.  $\square$

When the graph, embodied by  $W = \tilde{A}^T \tilde{A}$ , is ideal (Definition 2), ignoring or keeping the singular values makes no difference, since all of them are equal (by property 4 of Laplacian matrix and (21)). In this case, Rcut algorithm is equivalent to applying PCA to reduce the dimensionality of the data first, and then applying K-means to finish clustering. However, in practice, this condition can hardly be met even nearly, which essentially requires that after translating along a new dimension different clusters become near orthogonal. As a consequence, the indicator structure underlying the PCs may deviate much from the ideal one, and the singular values diverge. In this case, following exact PCA and applying K-means on the PCs,  $\Sigma_{1:K-1} V_{1:K-1}$ , may be preferable.

### 4.3 LE $\rightarrow$ PCA

**Proposition 7. (LE  $\rightarrow$  PCA)** *The objective of LE*

$$\min_{\tilde{X}} \text{tr}\{X L X^T\}, \text{ s. t. } X = \begin{bmatrix} \frac{1}{\sqrt{n}} \mathbf{1}^T \\ \tilde{X} \end{bmatrix}, X X^T = I, \quad (25)$$

where  $X \in \mathbb{R}^{r \times n}$ , can be converted to the form of dictionary representation

$$\min_{D, \tilde{X}} \|\tilde{A} - D X\|_F^2, \text{ s. t. } X = \begin{bmatrix} \frac{1}{\sqrt{n}} \mathbf{1}^T \\ \tilde{X} \end{bmatrix}, X X^T = I, \quad (26)$$

and further to the form of PCA

$$\min_{D, \tilde{X}} \|\tilde{A} - D \tilde{X}\|_F^2, \text{ s. t. } \tilde{X} \tilde{X}^T = I, \quad (27)$$

Let  $L = V^T \Lambda V$  be the spectral decomposition of  $L$ , where  $V_1 = \frac{1}{\sqrt{n}} \mathbf{1}^T$  and  $\lambda_n$  is the largest eigenvalue,  $\tilde{A}$  is defined as  $\tilde{A} = (\lambda_n I - \Lambda)^{\frac{1}{2}} V$ , called virtual data, and  $\bar{A}$  is the mean-removed version of  $\tilde{A}$ .

*Proof.* Since  $\lambda_n I - L = V^T (\lambda_n I - \Lambda) V = \tilde{A}^T \tilde{A}$ , we have

$$\min_X \text{tr}\{X L X^T\} \Leftrightarrow \max_X \text{tr}\{X (\lambda_n I - L) X^T\} = \max_X \text{tr}\{X \tilde{A}^T \tilde{A} X^T\}, \text{ s. t. } X X^T = I. \quad (28)$$

Further, by (18), (28) is equivalent to  $\min_X \|\tilde{A} - \tilde{A} X^T X\|_F^2$ , s. t.  $X X^T = I$ , and also  $\min_{D, X} \|\tilde{A} - D X\|_F^2$ , s. t.  $X X^T = I$ , with  $D^* = \tilde{A} X^{*T}$ . There remains minor difference to PCA:  $\tilde{A}$  is not mean-removed. We now tackle this problem. Since  $X = [\frac{1}{\sqrt{n}} \mathbf{1}, \tilde{X}^T]^T$ , the objective is equivalent to  $\min_{\tilde{X}} \|\tilde{A} (I - \frac{1}{\sqrt{n}} \mathbf{1} \frac{1}{\sqrt{n}} \mathbf{1}^T) (I - \tilde{X}^T \tilde{X})\|_F^2 = \min_{\tilde{X}} \|\bar{A} - \bar{A} \tilde{X}^T \tilde{X}\|_F^2$ , s. t.  $\tilde{X} \tilde{X}^T = I$ ,<sup>8</sup> where  $\bar{A} = \tilde{A} (I - \mathbf{1} \mathbf{1}^T / n)$  removes the mean of  $\tilde{A}$ . The objective finally is equivalent to (27), for  $D^* = \bar{A} \tilde{X}^{*T}$ .  $\square$

Keeping track of the eigenvectors of  $L$  during the conversions, and by the Eckart-Young theorem, we have

**Corollary 8.** *The solutions of  $\tilde{X}$  in (25), (26), and (27) are equivalent, one of them is  $V_{2:r}$ .*

### 4.4 Rcut $\rightarrow$ K-means

**Proposition 9. (Rcut  $\rightarrow$  K-means)** *The objective of Rcut*

$$\min_X \text{tr}\{X L X^T\}, \text{ s. t. } X \in \mathcal{H}, \quad (29)$$

can be converted to the form of K-means

$$\min_{D, \tilde{X}} \|\tilde{A} - D X\|_F^2, \text{ s. t. } X \in \mathcal{H}, \quad (30)$$

where  $\tilde{A}$  is defined as Proposition 7.

The conversion resembles last section except that an additional constraint  $X \in \mathcal{H}$  is added. The proof is omitted. At last, we also have

**Corollary 10.** *The solutions of  $X$  in (29) and (30) are equivalent, whereas the algorithmic results of applying Rcut to (29) and applying K-means to (30) may be different. Rcut algorithm relaxes (29) to (14), and applies K-means algorithm on the leading  $K$  normalized PCs of  $\tilde{A}$ , while K-means algorithm works with the full PCs, faithfully following the objective.*

<sup>8</sup>In precise, it holds when  $r \geq$  the null-space dimension of  $L$  so that  $\mathbf{1}$  must be a component of the solution.

## 5 Unification of PCA, K-means, LE, and Rcut

In Section 4, the bilateral relations between PCA and LE, K-means and Rcut have been established. Now, under the ideal graph condition (Definition 2), we will establish the equivalence of LE and Rcut, and then the equivalence of PCA and K-means is automatically established. Therefore, the four methods are unified together. Roughly speaking, the fundamental principle of the unification lies in that, under the condition, the indicator vectors become the leading singular vectors, which means the target of the cluster analysis methods, K-means and Rcut, coincides with that of the dimensionality reduction methods, PCA and LE.

Given a data set, we have two choices: one is to work with the original data, the other is to work with the similarity matrix constructed from the data. Therefore the theory has two versions: a linear version and a kernel version. Both of the conditions of the two versions concern the similarity matrices. The similarity matrix of the kernel version is usually built by the K-Nearest Neighbor (KNN) graph or the  $\varepsilon$ -neighborhood graph with Gaussian kernel [64], while that of the linear version is defined by the Gram matrix of data, in fact built by linear kernel.<sup>9</sup>

We now go into details. By spectral graph theory [13, 45, 44], as elaborated in Section 3.3, under the ideal graph condition, the indicator vectors become the leading eigenvectors of the Laplacian matrix, so the equivalence of LE and Rcut is manifest.<sup>10</sup>

**Theorem 11. (LE  $\Leftrightarrow$  Rcut)** *If the ideal graph condition is satisfied and  $K = r$ , then the solution of LE (25),  $X^*$ , attached with  $\frac{1}{\sqrt{n}}\mathbf{1}$ , and the solution of Rcut (29),  $H^*$ , are related by a rotation transform:  $\exists R \in \mathbb{R}^{r \times r}$ ,  $R^T R = I$ , such that*

$$X^* = RH^*. \quad (31)$$

By Corollary 4, 6, and Theorem 11, we can obtain the linear version of the unification.

**Theorem 12. (Unification: linear version)** *Working with the original data, if the ideal graph condition is satisfied and  $K = r \leq \text{rank}(A) + 1$ , then the solution of PCA (16) and LE (17), e.g.,  $X^* = V_{1:r-1}$ , and the normalized indicator solution of K-means (22) and Rcut (23),  $H^*$ , are related by a rotation transform:  $\exists R \in \mathbb{R}^{r \times r}$ ,  $R^T R = I$ , such that*

$$\begin{bmatrix} \frac{1}{\sqrt{n}}\mathbf{1}^T \\ V_{1:r-1} \end{bmatrix} = RH^*. \quad (32)$$

The theorem establishes the exact equivalence of PCA and K-means, together with the condition when it holds. Finally, by Corollary 8, 10, and Theorem 11, the kernel version of the unification is obtained.

**Theorem 13. (Unification: kernel version)** *Working with the similarity matrix, if the ideal graph condition is satisfied and  $K = r$ , then the solution of LE (25) and PCA (27), e.g.,  $\tilde{X}^* = V_{2:r}$ , and the normalized indicator solution of Rcut (29) and K-means (30),  $H^*$ , are related by a rotation transform:  $\exists R \in \mathbb{R}^{r \times r}$ ,  $R^T R = I$ , such that*

$$\begin{bmatrix} \frac{1}{\sqrt{n}}\mathbf{1}^T \\ V_{2:r} \end{bmatrix} = RH^*. \quad (33)$$

A diagram of the framework is shown in Figure 2.

## 6 Spectral Sparse Representation (SSR)

Under the ideal graph condition, PCA/LE, K-means/Rcut are unified. When this condition is met nearly but may not exactly, it leads to SSR (cf. Figure 2).

We provide a brief overview first. Ignoring minor factors, PCA and LE can be written in a form that finds a dictionary and codes to approximately represent the data:

$$\min_{D, X} \|A - DX\|_F^2, \text{ s. t. } XX^T = I, \quad (34)$$

where  $A$  is either transformed from the original data or factored from the Laplacian matrix. K-means and Rcut additionally impose the indicator constraint on  $X$ . Let  $A = U\Sigma V$ , one solution of PCA/LE is  $X^* = V_{1:r}$ , and any

<sup>9</sup>The two versions can be integrated into one general kernel version, which works with a similarity matrix that can be built by linear kernel, nonlinear kernel, or any other nonnegative and symmetric similarity measure. However, to make things clear, we distinguish them.

<sup>10</sup>By the same rationale, there is a counterpart in the literature [4], i.e., normalized LE and Ncut.

rotation of these eigenvectors constitutes a solution. When the graph is ideal, some rotation of the eigenvectors turns into indicator vectors (assume  $H^*$ ),  $V_{1:r} = RH^*$ . Thus PCA/LE, K-means/Rcut are unified, and the data can be represented as  $A \approx D^*V_{1:r} = \tilde{D}H^*$ , where  $D^* = AV_{1:r}^T$ ,  $\tilde{D} = AH^{*T}$ . The first representation form  $D^*V_{1:r}$  is of PCA/LE, while the second  $\tilde{D}H^*$  is of K-means/Rcut. When the graph is nearly ideal, the rotation of eigenvectors can only lead to noisy indicator vectors (assume  $H$ ),  $V_{1:r} = RH$ . When the data is represented by these noisy indicator vectors, which we call sparse codes, we have  $A \approx D^*V_{1:r} = \hat{D}H$ , where  $\hat{D} = AH^T$ . The representation form  $\hat{D}H$  is the spectral sparse representation.

SSR can be seen as a new representation method. It represents data in a dimensionality reduced way while achieving the same representation fidelity as PCA/LE. Meanwhile, the codes are sparse and approximate to the optimal indicator matrix of K-means/Rcut, so the underlying cluster structure can be revealed. In contrast to the hard clustering nature of K-means/Rcut, SSR is soft and descriptive. It describes the underlying clusters as well as the overlapping status of them. SSR lies in the intermediate of the two kinds of methods and combines some of the merits of both sides.

The perturbed indicator matrix is called sparse codes, since each column of it corresponds to a data point and is usually dominated by a single entry. A measure of sparsity can be defined as follows. For a vector  $x \in \mathbb{R}^n \neq \mathbf{0}$ ,

$$\text{sparsity}(x) = \|x\|_2 / \|x\|_1. \quad (35)$$

$1/\sqrt{n} \leq \text{sparsity}(x) \leq 1$ . The higher the value, the sparser the vector. The minimum is achieved when the magnitudes of the entries are uniform. The indicator matrix has only one nonzero entry in each column, achieving the maximum sparsity 1.

We provide a qualitative interpretation of the cluster information revealed by the sparse codes. The values of the code vector suggest how likely the data point belongs to different clusters. 1) If there is only one positive entry, then the index of it indicates its cluster membership. 2) If there are several positive entries, then the data is an overlapping point of some clusters. 3) If the sizes of the clusters are similar, the larger the entry is, the closer the point is to the corresponding cluster. We now analyze. Assume there are two clusters  $C_1$  and  $C_2$ , and exactly one overlapping point  $A_m$ . From the view of LE, we are to minimize  $\sum_{i,j} \|X_i - X_j\|^2 W_{ij}$ , s. t.,  $XX^T = I$ . There is a sub term  $\sum_{i \in \mathcal{N}_m} \|X_m - X_i\|^2 W_{mi}$  ( $\mathcal{N}_m$  is the neighborhood of  $A_m$ ), which requires that  $X_m^* = H_m$ , should be close to both  $[1/\sqrt{n_1}, 0]^T$  and  $[0, 1/\sqrt{n_2}]^T$  (ideal indicator vectors of neighboring points). Hence there will be a positive value in each row of  $H_m$ , with magnitudes less than  $1/\sqrt{n_1}$  and  $1/\sqrt{n_2}$  respectively. In order to meet the orthogonality between rows of  $H$ , small negative values must appear in the other columns of  $H$ . This is our first impression to the sparse codes.

SSR has two versions: the linear version (SSRl) and the kernel version (SSRk).

## 6.1 Kernel Version (SSRk): Similarity Matrix as Input

For convenience, we repeat some formulations. Let  $L = V^T \Lambda V$ , where  $V_1 = \frac{1}{\sqrt{n}} \mathbf{1}^T$ ,  $\lambda_1 = 0$  and  $\lambda_n$  is the largest eigenvalue. Define virtual data  $\tilde{A} = (\lambda_n I - \Lambda)^{\frac{1}{2}} V$ . LE is equivalent to

$$\min_{D \in \mathbb{R}^{n \times r}, X \in \mathbb{R}^{r \times n}} \|\tilde{A} - DX\|_F^2, \text{ s. t. } XX^T = I. \quad (36)$$

The solution set includes  $X^* = V_{1:r}$ ,  $D^* = \tilde{A}V_{1:r}^T$ , and any rotation of them.

**Theorem 14.** (SSRk) *When the graph is nearly ideal, there is a sparse representation*

$$\tilde{A} \approx \hat{D}H = \tilde{A}(H^T H). \quad (37)$$

*The approximation accuracy is optimal in the Frobenius-norm sense.  $H$  is the matrix of sparse codes, i.e., noisy indicator matrix, which satisfies*

$$V_{1:r} = RH, \quad (38)$$

*for some rotation matrix  $R$ .  $\hat{D}$  is a dictionary defined as*

$$\hat{D} = \tilde{A}H^T = \tilde{A}V_{1:r}^T R = \begin{bmatrix} (\lambda_n I - \Lambda_{1:r})^{\frac{1}{2}} R \\ \mathbf{0} \end{bmatrix} \approx \begin{bmatrix} \lambda_n^{\frac{1}{2}} R \\ \mathbf{0} \end{bmatrix}, \quad (39)$$

which has property  $\hat{D}^T \hat{D} \approx \lambda_n I$ , i.e., the atoms of  $\hat{D}$  are near-orthogonal and have similar lengths. The Gram matrix of codes  $H^T H \in \mathbb{R}^{n \times n}$  reflects the linear relationship of data, which has property

$$\mathbf{1}^T H^T H = \mathbf{1}^T V_{1:r}^T V_{1:r} = \mathbf{1}^T, \quad (40)$$

i.e., the sum of each column is one.

*Proof.* The key lies in (38), the others are easy to obtain. Assume the graph is ideal, and the underlying normalized indicator matrix is  $H^*$ . According to the properties of Laplacian matrix in Section 3.3,  $H^*$  spans the eigenspace of eigenvalue 0, and vector  $\mathbf{1}$  always belongs to this space. Define  $\tilde{V} = RH^*$ , then  $\tilde{V}$  remains to be the ideal eigenvectors of eigenvalue 0, where  $R$  is a rotation matrix so that  $\tilde{V}_1 = \frac{1}{\sqrt{n}} \mathbf{1}^T$ . Assume the graph becomes noisy. According to the matrix perturbation theory, the eigenvalues become  $\Lambda_{1:r} \approx \mathbf{0}$ , and the eigenvectors  $V_{1:r}$  becomes a perturbed version of  $\tilde{V}$ , i.e.,  $V_{1:r} = RH^* + E$ , where  $E$  is some noise. Then we obtain the relationship (38), where  $H = H^* + R^T E$  is the noisy indicator matrix.

If  $V_{1:r}$  and  $D^* = \tilde{A} V_{1:r}^T$  are a solution of (36), then the rotated version  $H = R^T V_{1:r}$  and  $\hat{D} = D^* R = \tilde{A} H^T$  are also a solution. Thus we obtain SSRk (37). The approximation accuracy is optimal in the Frobenius-norm sense, as indicated by the Eckart-Young theorem. Substituting the definition of  $\tilde{A}$  into  $\tilde{A} V_{1:r}^T R$ , we obtain the third equality of (39). The fourth approximation holds, due to  $\Lambda_{1:r} \approx \mathbf{0}$ . Finally, since  $V_{1:r}$  is orthonormal and  $V_1 = \frac{1}{\sqrt{n}} \mathbf{1}^T$ , (40) is obtained.  $\square$

SSRk has the following interpretations (it would be better to compare with those of PCA and K-means in Section 3.1 and Section 3.2 respectively):

1. The data can be sparsely represented by the dictionary.  $\tilde{A}_i \approx \hat{D} H_i$ , i.e.,  $\tilde{A}_i$  is approximated by a linear combination of a few atoms of dictionary  $\hat{D}$ .
2. The dictionary comes from the data clusters.  $\hat{D}_k = \tilde{A} H_k^T$ , implying  $\hat{D}_k$  mainly comes from the linear combination of samples in cluster  $C_k$ .  $\hat{D}_k$  can be seen as a quasi cluster center. However, compared with K-means, firstly, the weights are not uniform. They distribute according to the relevance of the data to the center. Moreover, the weights include small negative values, which imply least relevance. Secondly, since  $\hat{D}^T \hat{D} \approx \lambda_n I$ , the dictionary is incoherent, a desirable property in compressed sensing [9], and the mutual coherence  $\mu(\hat{D}) = \max_{i \neq j} |\hat{D}_i^T \hat{D}_j| / (\|\hat{D}_i\|_2 \cdot \|\hat{D}_j\|_2)$  is about zero.
3. The data are eventually represented by the data themselves according to relevance.  $\tilde{A}_i \approx \tilde{A} (H^T H_i)$ , implying  $\tilde{A}_i$  can be represented by a linear combination of the relevant samples. The sum of the weights, including negative values, is always 1. This coincides with K-means.

There is another representation form analogous to the un-normalized indicator representation form of K-means, which we will call un-normalized SSR:

$$\tilde{A} \approx D_U H_U, \quad (41)$$

where  $D_U = \hat{D} S_H^{-1}$ ,  $H_U = S_H H$ , and  $S_H = \text{diag}(H \mathbf{1})$ .  $H_U$  is the analogy of un-normalized indicator matrix, for  $\mathbf{1}^T H_U = \mathbf{1}^T$  as can be verified by (40).  $D_U$  are the proper cluster centers, as  $D_U = \tilde{A} (H^T S_H^{-1})$  and  $\mathbf{1}^T H^T S_H^{-1} = \mathbf{1}^T$ , i.e., the weights sum to 1.

## 6.2 Linear Version (SSRI): Original Data as Input

After turning PCA (16) to LE (17), we turn it back to the dictionary representation form:<sup>11</sup>

$$\min_{D \in \mathbb{R}^{(p+1) \times r}, X \in \mathbb{R}^{(r-1) \times n}} \|\tilde{A} - D \tilde{X}\|_F^2, \text{ s. t. } \tilde{X} = \begin{bmatrix} \frac{1}{\sqrt{n}} \mathbf{1}^T \\ X \end{bmatrix}, \tilde{X} \tilde{X}^T = I. \quad (42)$$

By the SVD of  $\tilde{A}$ , (20), the solution set includes  $\tilde{X}^* = \tilde{V}_{1:r} = \begin{bmatrix} \frac{1}{\sqrt{n}} \mathbf{1}^T \\ V_{1:r-1} \end{bmatrix}$ ,  $D^* = \tilde{A} \tilde{V}_{1:r}^T$ , and any rotation of them.

<sup>11</sup>First turn (17) back to the second line of (19), and then by (18), it leads to (42).

**Theorem 15. (SSRI)** When the graph is nearly ideal, there is a sparse representation

$$A \approx \hat{D}H = A(H^T H). \quad (43)$$

The approximation accuracy is optimal in the Frobenius-norm sense.  $H \in \mathbb{R}^{r \times n}$  ( $r \leq \text{rank}(A) + 1$ ) is the matrix of sparse codes, i.e., noisy indicator matrix, which satisfies

$$\begin{bmatrix} \frac{1}{\sqrt{n}} \mathbf{1}^T \\ V_{1:r-1} \end{bmatrix} = RH, \quad (44)$$

for some rotation matrix  $R$ .  $\hat{D} \in \mathbb{R}^{p \times r}$  is a dictionary defined as

$$\hat{D} = AH^T = A \left[ \frac{1}{\sqrt{n}} \mathbf{1}, V_{1:r-1}^T \right] R = U_{1:r-1} \Sigma_{1:r-1} R_{2:r}, \quad (45)$$

where  $R_{2:r}$  denotes the second to the  $r$ th rows of  $R$ . The Gram matrix of codes  $H^T H \in \mathbb{R}^{n \times n}$  reflects the linear relationship of data, which has property  $\mathbf{1}^T H^T H = \mathbf{1}^T \tilde{V}_{1:r}^T \tilde{V}_{1:r} = \mathbf{1}^T$ , i.e., the sum of each column is one.

*Proof.* Following similar reasoning of SSRk, (44) can be obtained, and there is a sparse representation of the augmented data:  $\tilde{A} \approx \tilde{D}H = \tilde{A}H^T H$ , where by the SVD of  $\tilde{A}$ , (20), and (44),  $\tilde{D} = \tilde{A}H^T = \begin{bmatrix} 1 \\ U_{1:r-1} \end{bmatrix} \begin{bmatrix} \sqrt{\beta n} \\ \Sigma_{1:r-1} \end{bmatrix} R$ .

We now focus on (43), where the representation is for the *original data*. First, we reduce (42) to a form that involves only the original data. Substituting  $D = \tilde{A}\tilde{X}^T$  into (42), note that the first row of  $\tilde{A}\tilde{X}^T\tilde{X}$  is always  $\sqrt{\beta}\mathbf{1}^T$ , equal to the first row of  $\tilde{A}$ . Thus we can remove this artificial component:

$$\min_{\tilde{D} \in \mathbb{R}^{p \times r}, X} \|A - \tilde{D}\tilde{X}\|_F^2, \text{ s. t. } \tilde{X} = \begin{bmatrix} \frac{1}{\sqrt{n}} \mathbf{1}^T \\ X \end{bmatrix}, \tilde{X}\tilde{X}^T = I. \quad (46)$$

The solution of the codes remains the same. Hence, we have  $A \approx \tilde{D}^* \tilde{X}^* = A \tilde{X}^{*T} \tilde{X}^*$ . Combining with the solution of (42), and (44), we obtain SSRI (43). Finally it is easy to verify that (45) holds.  $\square$

Though augmenting  $X$  with a constant component  $\frac{1}{\sqrt{n}}\mathbf{1}$ , (46) is equivalent to PCA (16), due to  $A\mathbf{1} = \mathbf{0}$  and  $\|A(I - \tilde{X}^T \tilde{X})\|_F^2 = \|A(I - \frac{1}{\sqrt{n}}\mathbf{1} \frac{1}{\sqrt{n}}\mathbf{1}^T)(I - X^T X)\|_F^2 = \|A(I - X^T X)\|_F^2$ . However, PCA cannot explicitly reveal the cluster structure, because in the absence of the redundant  $\frac{1}{\sqrt{n}}\mathbf{1}$ , the sparse codes cannot be recovered through rotating  $V_{1:r-1}$  only.

The interpretations are similar to those of SSRk and an un-normalized SSRI exists, except that the dictionaries are usually not near-orthogonal. This is because the singular values are not uniform, which usually decay very fast. The more fundamental reason underlying this phenomenon is that, as argued before, the ideal graph condition essentially requires that after translating along a new dimension the clusters become orthogonal, which can hardly be met in practice, except perhaps for some high-dimensional data. Nevertheless, linear models, as elementary components in the family of machine learning, usually lay down important parts of the theoretical foundation and provide support for more advanced methods, therefore should not be underestimated.

Finally, we mention that the virtual data in the kernel version and the augmented data including the auxiliary constant  $\beta$  in the linear version would not play actual roles in practice, their functions are to establish theory and facilitate understanding. However, the constant vector  $\mathbf{1}$  discarded by dimensionality reduction indeed is indispensable for revealing cluster structure and therefore plays essential roles in SSR and cluster analysis.

### 6.3 SSR for Out-of-sample Data

Within unsupervised learning domain, SSR solves sparse codes for a given sample set. When new data (called out-of-sample data) come, solving the sparse codes of them is not necessarily straightforward, especially for the kernel version [6]. To make SSR fully useful, we have to be able to address this problem.



### 6.3.1 Kernel Version

There are some prior work dealing with the out-of-sample problem for Ncut [6, 5]. However, the kernel function of LE/Rcut is different, we will solve the problem in our context.

Given a new point  $b$ , we denote its out-of-sample LE codes by  $V_b \in \mathbb{R}^r$ , and its sparse codes by  $H_b$ . By the rotation relation between sparse codes and codes of LE (38), if we can get  $V_b$ , then  $H_b$  can be obtained using the same rotation matrix:

$$H_b = R^T V_b. \quad (47)$$

First, we study the ideal case, and solve  $V_b$ .

**Theorem 16.** *Given a new point  $b$  with similarities to the data set  $W_b = [W_{1,b}, \dots, W_{n,b}]^T$ , and denoting the sum of  $W_b$  by  $s_b$ , if the ideal graph condition is satisfied and  $b$  is not an overlapping point, then  $b$ 's LE codes are*

$$V_b = (s_b I - \Lambda_{1:r})^{-1} V_{1:r} W_b, \quad (48)$$

or, since  $\Lambda_{1:r} = \mathbf{0}$ ,

$$V_b = V_{1:r} (W_b / s_b). \quad (49)$$

*Proof.* By assumption and properties of Laplacian matrix,  $\tilde{H} = [H, H_b]$  are eigenvectors of the augmented Laplacian matrix:

$$\tilde{L} = \begin{bmatrix} \tilde{S} - W & -W_b \\ -W_b^T & s_b \end{bmatrix}. \quad (50)$$

That is  $\tilde{L} \tilde{H}^T = \tilde{H}^T \Lambda_{1:r}$ .  $\Lambda_{1:r}$  are virtually zero, so we also have  $\tilde{L} \tilde{H}^T R^T = \tilde{H}^T R^T \Lambda_{1:r}$ , which implies  $\tilde{V}_{1:r} = R \tilde{H} = [V_{1:r}, V_b]$  are also eigenvectors. We see that the eigenvectors of sample set,  $V_{1:r}$ , are preserved during the extension. Substituting (50) into  $\tilde{L} \tilde{V}_{1:r}^T = \tilde{V}_{1:r}^T \Lambda_{1:r}$  and considering the last row, we have  $-W_b^T V_{1:r}^T + s_b V_b^T = V_b^T \Lambda_{1:r}$ . Therefore, (48) is obtained.  $\square$

When the graph is nearly ideal, we will still estimate the LE codes by (48).<sup>12</sup> Further, since  $\Lambda_{1:r} \approx \mathbf{0}$ , especially orders of magnitude smaller than  $s_b$  in practice, we can still use (49) as approximation. By (47), finally we have:

**Theorem 17.** *The sparse codes of  $b$  can be estimated as*

$$H_b = H (W_b / s_b). \quad (51)$$

Both (49) and (51) have very clear interpretation: the out-of-sample codes are obtained by the weighted combination of the codes of sample set, and the weights are nonnegative and sum to 1. Besides, note that when the graph is ideal, replacing the new data with sample set, (49) and (51) lead to exactly the sample-set codes,  $V_{1:r}$  and  $H$ . This is due to the properties of normalized Laplacian matrix  $S^{-1}W$ , cf. footnote 12. Finally, as the derivation does not depend on the row-length of  $H$ , if we use un-normalized SSR (41), there is an alternative:  $H_b = H_U (W_b / s_b)$ , and  $\mathbf{1}^T H_b = 1$  too.

### 6.3.2 Linear Version

This version is simpler, since the out-of-sample codes of PCA is easy to obtain, and a rotation of it leads to sparse codes. Nevertheless, we investigate it systematically for deeper understanding.

First, note the solution of the linear regression problem:

$$\min_{D_T \in \mathbb{R}^{r \times (p+1)}} \|\tilde{X} - D_T \tilde{A}\|_F^2. \quad (52)$$

$(D_T)^* = \tilde{X} \tilde{A}^\dagger$ . When  $\tilde{X}$  is the normalized PCs,  $\tilde{V}_{1:r}$ , by the SVD of  $\tilde{A}$  (20),  $(D_T)^* = \tilde{\Sigma}_{1:r}^{-1} \tilde{U}_{1:r}^T = (D^*)^\dagger$  and  $\tilde{X} = (D_T)^* \tilde{A}$ , where  $D^*$  is the solution of (42). Similarly, when  $\tilde{X}$  is the sparse codes,  $H$ , we have solution  $\hat{D}_T = R^T \tilde{\Sigma}_{1:r}^{-1} \tilde{U}_{1:r}^T = \hat{D}^\dagger$ , and  $\tilde{X} = \hat{D}_T \tilde{A}$ , where  $\hat{D}$  is the dictionary of SSRI. The two dictionaries are related by a rotation  $\hat{D}_T = R^T (D_T)^*$ , which is the counterpart of  $\hat{D} = D^* R$ . The above principle suggests that

<sup>12</sup>When  $s_b = 0$ , as the sample set of kernel PCA satisfy, (48) reduces to the out-of-sample codes of kernel PCA [57]. Besides, similar results can be obtained by studying the normalized Laplacian matrix  $S^{-1}W$  (or optionally applying the Nyström formula [66, 5]), since the eigenvectors of  $L$  with eigenvalue zero (smallest) are the eigenvectors of  $S^{-1}W$  with eigenvalue one (largest) [64]. (48) will be replaced with  $V_b = (I - \Lambda_{1:r})^{-1} V_{1:r} (W_b / s_b)$ , while (48) remains unchanged.

**Theorem 18.** Given a new point  $b$  (with mean removed as  $A$ ), and denoting its augmented data by  $\tilde{b} = [\sqrt{\beta}, b^T]^T$ , then its augmented PCA codes and sparse codes can be obtained by

$$\tilde{V}_b = (D^*)^\dagger \tilde{b} = \begin{bmatrix} \frac{1}{\sqrt{n}} \\ \Sigma_{1:r-1}^{-1} U_{1:r-1}^T b \end{bmatrix}, \quad (53)$$

$$H_b = \hat{D}^\dagger \tilde{b} = R^T \tilde{V}_b. \quad (54)$$

The proof of the final expression of  $\tilde{V}_b$  involves tedious expansion of  $\tilde{A}$ 's SVD (20), which we will omit. Note that,  $\Sigma_{1:r-1}^{-1} U_{1:r-1}^T b$  is exactly the PCA codes of  $b$ , and the auxiliary constant  $\beta$  does not play actual role. Besides, by the orthonormality of  $\tilde{V}_{1:r}$  and  $H$ , we have:

**Corollary 19.**

$$\tilde{V}_b = \begin{bmatrix} \frac{1}{\sqrt{n}} \\ V_b \end{bmatrix}. \quad (55)$$

The out-of-sample codes can also be written in terms of sample-set codes:  $\tilde{V}_b = \tilde{V}_{1:r}(\tilde{V}_{1:r}^T \tilde{V}_b)$ ,  $H_b = H(\tilde{V}_{1:r}^T \tilde{V}_b)$ , where vector  $\tilde{V}_{1:r}^T \tilde{V}_b = \frac{1}{n} \mathbf{1} + V_{1:r}^T V_b$  and  $\mathbf{1}^T (\tilde{V}_{1:r}^T \tilde{V}_b) = 1$ .

The corollary implies that the out-of-sample codes is a weighted combination of the codes of sample set. The weights are similarities defined by the inner product of PCs, and they sum to 1. These expressions are consistent with those of kernel version. Original codes can be recovered by replacing the new data with sample set, and an alternative by normalizing  $H_b$  to sum 1 exists. Finally, in view of (53) and (54), the codes can be directly obtained by applying a linear transform to the data. It implies that SSR1 is both synthesis SR and analysis SR/sparsifying transform [26, 46, 52].

## 6.4 NSCrT: to Solve Sparse Codes

To make SSR practical, we have to find the rotation matrices in (38) and (44) accurately. (38) or (44) essentially requires to find a rotation matrix and sparse codes such that the sparse codes match the normalized PCs after the rotation. We employ a modified version of SPCArt [36] to accomplish this task. SPCArt is a sparse PCA algorithm designed to solve sparse loadings. It finds a rotation matrix and sparse loadings such that the sparse loadings approximate the PCA loadings after the rotation. Replacing the PCA loadings with the normalized PCs, SPCArt meets our need. Considering our sparse codes are noisy indicators, the dominant values of which are nonnegative, we additionally impose nonnegative constraint on the codes. The modified algorithm is called NSCrT (nonnegative sparse coding via rotation and truncation).

Given a row-wise orthonormal matrix  $X \in \mathbb{R}^{r \times n}$ , the objective of NSCrT is

$$\min_{R \in \mathbb{R}^{r \times r}, \bar{H} \in \mathbb{R}^{r \times n}} \|X - R\bar{H}\|_F^2 + \lambda^2 \|\bar{H}\|_0, \text{ s. t. } R^T R = I, \bar{H}_{ij} \geq 0, \forall i, j, \quad (56)$$

where  $R$  is the rotation matrix,  $\bar{H}$  is the matrix of truncated sparse codes,  $\|\bar{H}\|_0$  counts the number of nonzero entries of  $\bar{H}$ ,  $\lambda$  is a small threshold in  $(0, 1)$ . Since we want to find an equivalence relation between  $X$  and  $R\bar{H}$ , as (38) and (44) require, rather than an approximation relation, after  $R$  is solved, we obtain sparse codes as  $H = R^T X$ .

Note (56) itself is a dictionary learning problem, but the characteristics of its operands make the solution elegant. Following SPCArt, a local optimum can be solved by alternately optimizing  $R$  and  $\bar{H}$ . When initializing  $R = I$ , the solution process results into operations of alternately rotating and truncating  $X$ .

1) Fixing  $R$ , (56) becomes

$$\min_{\bar{H}} \|R^T X - \bar{H}\|_F^2 + \lambda^2 \|\bar{H}\|_0, \text{ s. t. }, \bar{H}_{ij} \geq 0, \forall i, j. \quad (57)$$

Denote  $H = R^T X$ , note that  $H$  is a rotation of  $X$ , which is orthonormal and spans the same subspace as  $X$ . It is not hard to see that the solution of  $\bar{H}$  is:  $\bar{H}_{ij}^* = H_{ij}$  if  $H_{ij} \geq \lambda$ , and  $\bar{H}_{ij}^* = 0$  otherwise, i.e., it is obtained by truncating small values of  $H$  that are below  $\lambda$ .

2) Fixing  $\bar{H}$ , (56) becomes a Procrustes problem

$$\min_R \|X\bar{H}^T - R\|_F^2, \text{ s. t. } R^T R = I. \quad (58)$$

---

**Algorithm 1** NSCrT for solving sparse codes

---

**Input:**

row-wise orthonormal eigenvectors  $X \in \mathbb{R}^{r \times n}$ , threshold  $\lambda \in (0, 1)$

**Output:**

sparse codes  $H \in \mathbb{R}^{r \times n}$  and its truncated version  $\bar{H}$ , rotation matrix  $R \in \mathbb{R}^{r \times r}$

- 1: Initialize  $R$ :  $R \leftarrow I$
  - 2: **repeat**
  - 3:   Rotation:  $H \leftarrow R^T X$
  - 4:   Truncation:  $\forall i, j, \bar{H}_{ij} \leftarrow H_{ij}$  if  $H_{ij} \geq \lambda$ , and  $\bar{H}_{ij} \leftarrow 0$  otherwise
  - 5:   Update  $R$ : compute SVD of  $X \bar{H}^T$ :  $U \Sigma V$ , then  $R \leftarrow UV$
  - 6: **until** convergence
  - 7: Obtain final sparse codes:  $H \leftarrow R^T X$
- 

---

**Algorithm 2** SSR of kernel version (SSRk)

---

**Input:**

similarity matrix  $W \in \mathbb{R}^{n \times n}$ , code dimension  $r$ , threshold  $\lambda$ , out-of-sample similarity vector  $W_b \in \mathbb{R}^n$  (optional)

**Output:**

sparse codes  $H \in \mathbb{R}^{r \times n}$ , rotation matrix  $R \in \mathbb{R}^{r \times r}$ , out-of-sample sparse codes  $H_b \in \mathbb{R}^r$  (optional)

- 1: Compute Laplacian matrix:  $L \leftarrow \text{diag}(W\mathbf{1}) - W$
  - 2: Compute the  $r$  smallest eigenvectors of  $L$ :  $V \in \mathbb{R}^{r \times n}$
  - 3: Solve sparse codes:  $\{H, R\} \leftarrow \text{NSCrT}(V, \lambda)$
  - 4: If  $W_b$  is provided,  $H_b \leftarrow HW_b / (\mathbf{1}^T W_b)$
- 

Let  $X \bar{H}^T = U \Sigma V$  be the SVD, then  $R^* = UV$ .

The NSCrT algorithm is presented in Algorithm 1, and those of SSRk and SSRI are presented in Algorithm 2 and Algorithm 3 respectively. The time complexity of NSCrT is  $O(nr^2)$ , which scales linearly with the data size. It is efficient if  $r$  is not too large.

## 6.5 Sparse Cut (Scut): Application of SSR in Clustering

As an application of SSR, the sparse codes  $H$  can be directly used for clustering. Since the sparse codes are noisy indicator vectors, where usually only one dominant value appears in each column, we can check the maximal entry in each column and assign its index as the cluster label:<sup>13</sup>

$$c_i \leftarrow \arg \max_k H_{ki}, 1 \leq i \leq n. \quad (59)$$

---

<sup>13</sup>There is a more concrete interpretation for Scut in the case of SSRk, details are included in Appendix A.

---

**Algorithm 3** SSR of linear version (SSRI)

---

**Input:**

mean-removed data set  $A \in \mathbb{R}^{p \times n}$ , code dimension  $r$  ( $r \leq \text{rank}(A) + 1$ ), threshold  $\lambda$ , mean-removed out-of-sample data  $b \in \mathbb{R}^p$  (optional)

**Output:**

sparse codes  $H \in \mathbb{R}^{r \times n}$ , rotation matrix  $R \in \mathbb{R}^{r \times r}$ , out-of-sample sparse codes  $H_b \in \mathbb{R}^r$  (optional)

- 1: Compute rank  $r - 1$  SVD of  $A$ :  $U \Sigma V$
  - 2: Solve sparse codes:  $\{H, R\} \leftarrow \text{NSCrT}\left(\begin{bmatrix} \frac{1}{\sqrt{n}} \mathbf{1}^T \\ V \end{bmatrix}, \lambda\right)$
  - 3: If  $b$  is provided,  $H_b \leftarrow R^T \begin{bmatrix} \frac{1}{\sqrt{n}} \\ \Sigma^{-1} U^T b \end{bmatrix}$
-

---

**Algorithm 4** Sparse cut (Scut)

---

**Input:**sparse codes  $H \in \mathbb{R}^{r \times n}$  output by SSR (or out-of-sample sparse codes)**Output:**cluster labels  $c \in \mathbb{N}^{1 \times n}$ 1:  $c_i \leftarrow \arg \max_{k=1, \dots, r} H_{ki}, i = 1, \dots, n$ 

---

We call this SSR based clustering, sparse cut (Scut), shown in Algorithm 4. In brief, combining with SSR, Scut performs the following steps: 1) compute the normalized PCs of data (SSRl), or the eigenvectors of Laplacian matrix (SSRk), 2) employ NSCrT to recover the noisy indicator vectors from the eigenvectors, 3) finish clustering by checking the maximal entries.

There is another alternative with minor difference: normalizing each column of  $H$  to sum 1 first, and then  $c_i \leftarrow \arg \max_k H_{ki}$ , where  $H_U$  is the code matrix of the un-normalized SSR (41). The quasi-probability interpretation of  $H_U$  justifies this scheme. The difference is: the first scheme weights the smaller clusters more, since  $1/\sqrt{n_i} < 1/\sqrt{n_j}$  if  $n_i > n_j$ , while the latter scheme treats them equally, since all columns sum to 1. This paper adopts the first scheme.

## 7 Experiments

The experiments consist of: 1) validating the ability of NSCrT in recovering rotation matrix, 2) illustration of the cluster structure revealed by sparse codes, 3) a comparison between the linear version and the kernel version, in terms of the ideal graph condition and clustering performance, 4) investigation of the relations between ideal graph condition, sparsity, and clustering accuracy, 5) the performance of kernel Scut, 6) comparison of the clustering performance between SSR and OSRs.

Table 2: Data sets.

Data set	Description	#Classes	Size	Sizes of classes
G1,G2,G3	three artificial Gaussian data with more and more heavy overlaps, shown in Figure 4	3	$2 \times 150$	50,50,50
onion	an artificial data of unbalanced classes, shown in Figure 6	3	$2 \times 75$	5,20,50
iris	Fisher's iris flower data set	3	$4 \times 150$	50,50,50
wdbc	breast cancer Wisconsin (diagnostic) data set	2	$30 \times 569$	212,357
Isolet	spoken (English) letter recognition data set, subset of the first set, excluding classes "c,d,e,g,k,n,s"	19	$617 \times 1140$	each 60
USPS3, USPS8, USPS10	three subsets of the training set of United States Postal Service (USPS) handwritten digit database. USPS3: "0"-"2", USPS8: excludes "5" and "9" (as "3" and "5", "4" and "9", "7" and "9" heavily overlap), USPS10: "0"-"9"	3,8,10	$256 \times 2930$ , $256 \times 6091$ , $256 \times 7291$	1194,1005,731, 658,652,556, 664,645,542,644
4News	four groups {2,9,10,15} of 20 Newsgroups documents, tf-idf sparse features are used	4	$26214 \times 2372$	389,398,397,394
TDT2	the largest 30 categories of NIST Topic Detection and Tracking corpus, documents appearing in more than one categories are removed, tf-idf sparse features are used	30	$36771 \times 9394$	1844,1828,1222, 811,...,52
polb	a relation network (sparse) of books about US Politics ("liberal", "conservative", or "neutral"), edges represent copurchasing of books by the same buyers	3	$105 \times 105$	43,49,13

The data sets we used, shown in Table2,<sup>14</sup> contain class labels for each sample, which serve as ground-truth for the evaluation. To make the evaluation with the class labels reasonable, the data sets are chosen so that the

<sup>14</sup>The sources of the public data sets are listed below.

iris: <http://archive.ics.uci.edu/ml/datasets/Iris>

Isolet: <http://archive.ics.uci.edu/ml/datasets/ISOLET>

wdbc: <http://archive.ics.uci.edu/ml/machine-learning-databases/breast-cancer-wisconsin/>

USPS: <http://www-i6.informatik.rwth-aachen.de/~keyser/usps.html>

TDT2: <http://www.nist.gov/speech/tdt98/tdt98.htm>

4News: <http://qwone.com/~jason/20Newsgroups/>

polb: <http://networkdata.ics.uci.edu/data.php?id=8>

underlying clusters of the data are in good accord with the man-assigned class labels. The data sets come from various domains and are of diverse nature. G1, G2, and G3 have more and more heavy cluster-overlaps. The class sizes of onion and TDT2 are highly unbalanced. The number of samples in USPS10 and TDT2 are large. 4News and TDT2 are high-dimensional data sets with  $p > n$ . 4News and TDT2 are sparse data. The number of classes in Isolet and TDT2 are relatively large. Polb is a relational data with only similarity matrix provided.

Clustering performance is measured by four criteria: 1) accuracy (percentage of total correctively classified points), 2) normalized mutual information (NMI) [43], 3) rand index (RI) [43], 4) time cost. For accuracy, the matching between the output clusters and the labeled classes is established by the Hungarian algorithm [38].

The algorithms are implemented using MATLAB, run on a PC with 2.93GHz duo core CPU, 2GB memory. The similarity matrices of the kernel version (except polb) are built by 4NN graph (4News uses 9NN to avoid isolated points) with the self-tuning method of [75]. For NSCrT, we set  $\lambda = 0.6/\sqrt{n}$ ,<sup>15</sup> 200 maximal iterations, and  $\|R^{(t)} - R^{(t-1)}\|_F/\sqrt{r} \leq 0.01$  to be the convergence condition. We observed it usually converged within a dozen iterations.

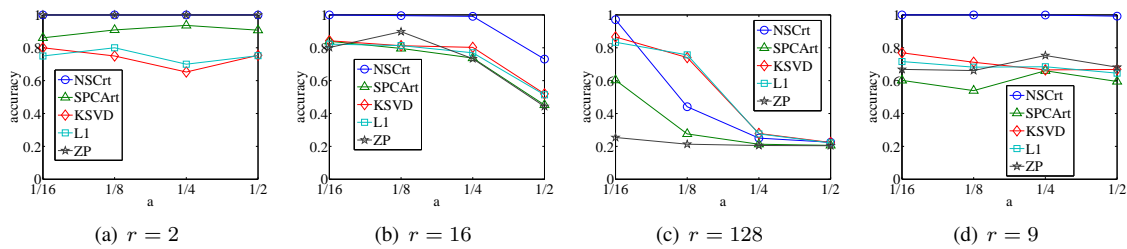


Figure 3: Accuracy of NSCrT in recovering rotation matrix. The horizontal axis indicates noise level. (a)-(c) data of uniform cluster-sizes. (d) data of exponential cluster-sizes.

## 7.1 Accuracy of NSCrT in Recovering Rotation Matrix

SSR is practical and Scut is feasible only if we can find the right rotation matrix, so we test the accuracy of NSCrT in recovering the rotation matrix first. Randomly generated rotation matrices and sparse codes are used for the test. The performance is compared with those of four other algorithms:  $\ell_0$ -norm based SPCArt [36], ZP [75], KSVD [2] and an  $\ell_1$ -norm based KSVD, denoted by “L1”.<sup>16</sup>

First, a rotation matrix  $R \in \mathbb{R}^{r \times r}$ , a normalized indicator matrix  $H^* \in \mathbb{R}^{r \times 1024}$ , and Gaussian noise  $E$  of mean zero are randomly generated. Then, data  $X$  is synthesized via  $X \leftarrow R(H^* + E)$ , where  $H^* + E$  simulates the sparse codes. We input  $X$  into the algorithms and test their accuracies in recovering  $R$ . Two kinds of data sets are generated. 1) Data of uniform cluster-sizes. Each row of  $H^*$  has the same number of nonzeros  $n_k = n/r$ ,  $1 \leq k \leq r$ , with entry value  $1/\sqrt{n_k}$ . Three number of clusters are tested:  $r = 2, 16, 128$ . 2) Data of exponential cluster-sizes.  $r = 9$ . The  $k$ th row ( $k < 9$ ) of  $H^*$  has  $n_k = 2^k$  nonzero entries with value  $1/\sqrt{n_k}$ , the last row has  $n_9 = (n - \sum_{k=1}^8 n_k)$  nonzero entries with value  $1/\sqrt{n_9}$ . Note that the smallest cluster has only 2 members, while the largest one has 514 members, the cluster sizes are highly unbalanced. For each case above, the algorithms are tested under increasing Gaussian noise  $\sigma = a \min_k 1/\sqrt{n_k}$ , where  $a$  is a factor relative to the smallest value of codes,  $a = 1/16, 1/8, 1/4, 1/2$ . On the highest level, the standard deviation of Gaussian has magnitude up to half of that of data.

The accuracy is measured by the mean of cosines between the estimated rotation  $\hat{R}$  and  $R$ :  $1/r \sum_{k=1}^r |\hat{R}_k^T R_k|$ , where the matching of columns is established by the Hungarian algorithm [38]. The mean accuracies over 20 runs are shown in Figure 3. We see that NSCrT outperforms the others. The improvement is most significant when the cluster sizes are unbalanced (Figure 3(d)), where the margin is more than 20%. Besides, NSCrT frequently obtains

<sup>15</sup>According to the performance-guarantee analysis in SPCArt [36], it is recommended to set  $\lambda$  around  $1/\sqrt{n}$ . In our case, we found  $\lambda = 0.6/\sqrt{n}$  consistently performed well.

<sup>16</sup>Codes of KSVD and ZP are downloaded from <http://www.cs.technion.ac.il/~ronrubin/software.html> and <http://www.vision.caltech.edu/lihi/Demos/SelfTuningClustering.html> respectively. KSVD and L1 are dictionary learning methods. They participate in the comparison for the recovery of  $R$  can be formulated as a dictionary learning problem under sparse representation framework, as NSCrT does. In KSVD, the  $\ell_0$ -norm of each sparse code-vector is constrained to be 1. For L1, the dictionary update step follows KSVD, while the sparse coding step adopts the  $\ell_1$ -norm based SLEP [41].

mean accuracies over 98%, which indicates the standard deviations are very small, in other words, the performance of NSCrT is stable. Note that although NSCrT intends to find local minima, in moderate noise level, it recovers the underlying solutions with high accuracy.

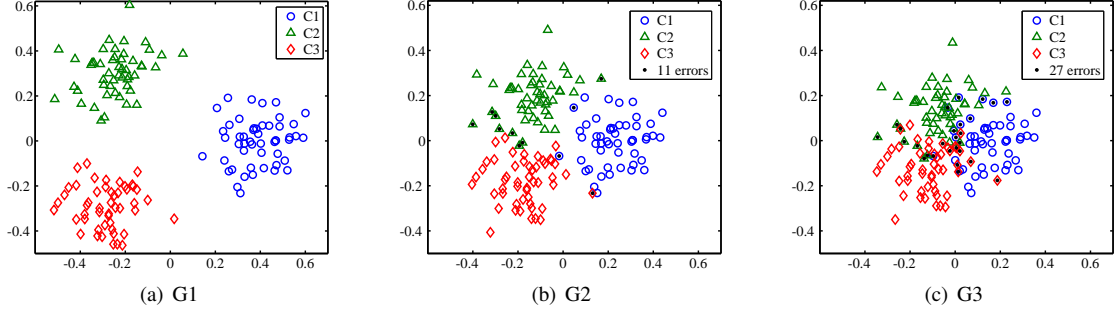


Figure 4: Gaussian data G1-G3 of different overlaps. Black dots indicate points misclassified by kernel Scut (see Section 7.2). These points lie on the overlapping regions.

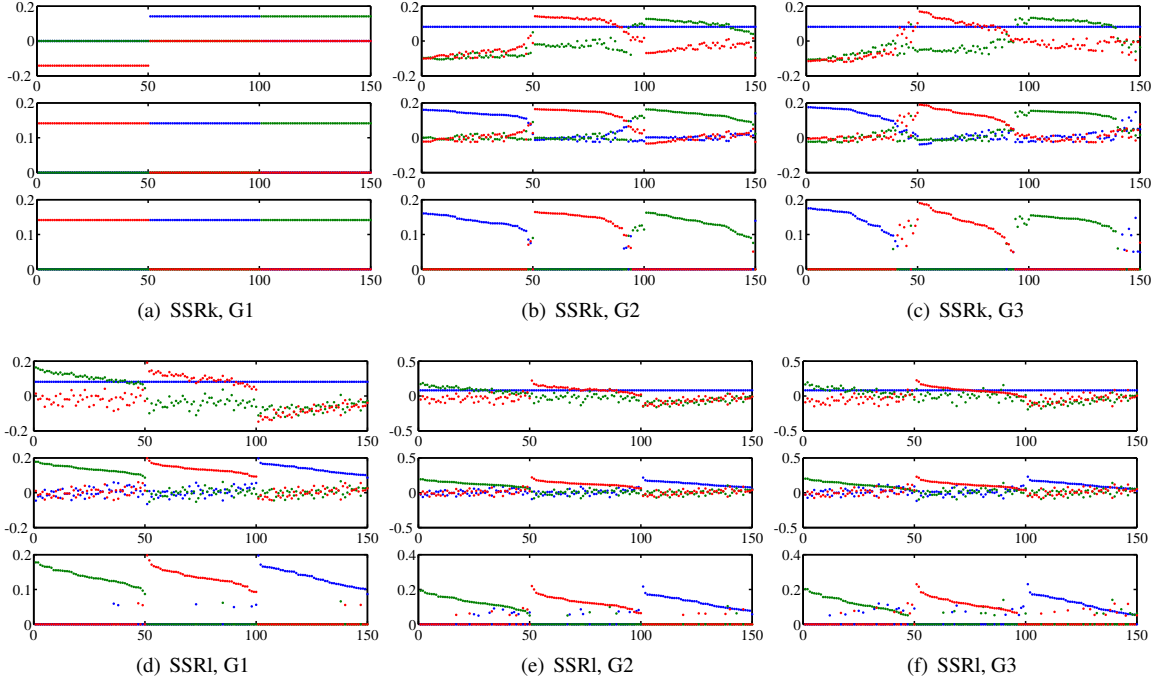


Figure 5: Row vectors of sparse codes of G1-G3. In each subfigure, top: eigenvectors  $V \in \mathbb{R}^{3 \times 150}$  (one color corresponds to one vector), middle: sparse codes  $H = R^T V$  obtained by NSCrT, bottom: truncated sparse codes  $\bar{H}$ . The three segments 1-50, 51-100, 101-150 on horizontal axis correspond to the three ground-truth clusters. Within each segment, samples are rearranged according to the confidence to its truth cluster.

## 7.2 Illustrations of Cluster Structure Revealed by Sparse Codes of SSR

It has been qualitatively analyzed how the sparse codes reveal cluster structure in Section 6. We now illustrate it from row perspective, column perspective, and Gram matrix perspective. The Gaussian data G1, G2, G3, and onion data are taken as examples. Both SSRk and SSRI are shown.

The row vectors of sparse codes  $H$  are demonstrated in Figure 5 and Figure 7. Usually, on each column of  $H$ , only one value dominates, which indicates the cluster membership. The cross sections of these vectors at the end

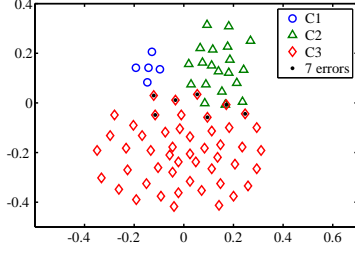


Figure 6: onion data: artificial data with unbalanced classes.

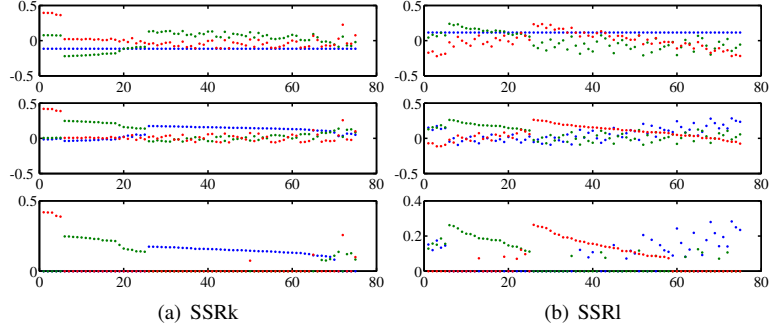


Figure 7: Row vectors of sparse codes of onion data. Interpretation is similar to that in Figure 5.

of each segment indicate the overlapping regions. In Figure 5, the cross sections become more and more significant from (a) to (c), faithfully reflecting the overlapping status. Samples in these cross sections will be misclassified by Scut, which are plotted as black dots in Figure 4 and Figure 6.

The column vectors of sparse codes, taking G2 as example, are illustrated in Figure 8. For SSRk, compared with the original data in Figure 4(b), the codes make the cluster structure prominent. Besides, in contrast to the 0-1 discrete codes of K-means, the sparse codes are continuous, which can describe the clusters (if one entry dominates) and the overlaps (if several comparable entries exist). The truncated sparse codes try to resolve the overlaps, being closer to the K-means's codes.

The Gram matrix  $H^T H$  reveals the linear relation of data: each sample can be approximated by the linear combination of all samples, with weights provided by the corresponding column of  $H^T H$ . Taking G2 as example, the matrices are shown in Figure 9. We see the weights in each column of  $H^T H$  distribute according to the relevance of the corresponding sample to all samples.  $\bar{H}^T \bar{H}$  removes the small weights, especially the negative ones, making the main relation clearer. For SSRk, the averages of column sums in  $\bar{H}^T \bar{H}$  on G1-G3 and onion are 1, 0.9866, 0.9249, and 0.9784 respectively, still close to 1, implying the distortions due to truncations are small.

Table 3: Linear version v.s. kernel version:  $\rho$  values ( $0 \leq \rho \leq 1$ ) of the similarity matrices. A higher value indicates the ideal graph condition is met better.

$\rho$ (%)	G1	G2	G3	onion	iris	wdbc	Isolet	USPS3	USPS8	USPS10	4News	TDT2
SSRI	20.1	15.8	12.7	15.2	1.3	13.2	0.1	2.2	1.0	0.1	4.0	0.04
SSRk	100.0	59.4	58.4	39.4	63.2	67.7	16.8	60.5	5.1	6.8	1.9	4.7

### 7.3 Linear Version v.s. Kernel Version

We first compare how well the ideal graph condition is met for the two versions qualitatively from the view of the structure of similarity matrix, and then propose a measure for quantitative evaluation. Finally we compare the clustering performance of the two versions.

First, a clearer block-diagonal structure of the similarity matrix indicates the condition is met better. The similarity matrices on some representative data sets are shown in Figure 10. We see that so long as the data has clear clusters, the similarity matrix of the kernel version will meet the condition well, but that of the linear version

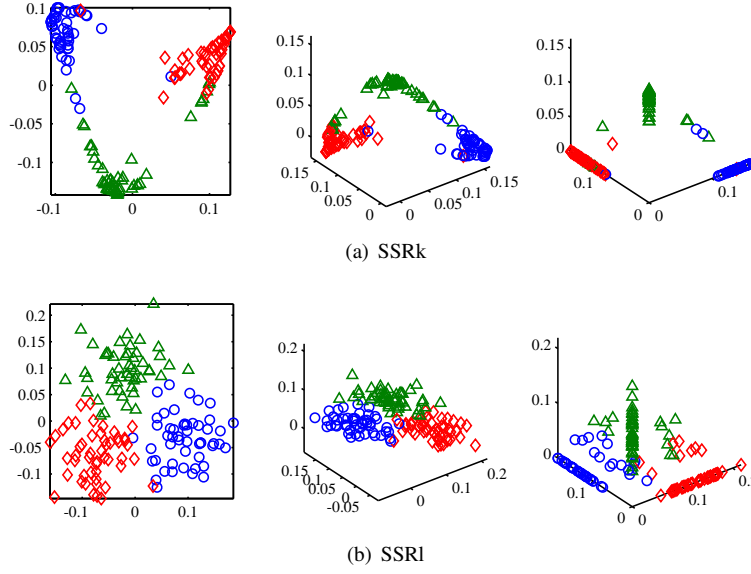


Figure 8: Column vectors of sparse codes  $H \in \mathbb{R}^{3 \times 150}$  of G2 data. One point corresponds to one sample. Left: intrinsic 2D manifold, i.e.,  $V_{2,3}$ , middle:  $H$ , right: truncated sparse codes  $\bar{H}$ .

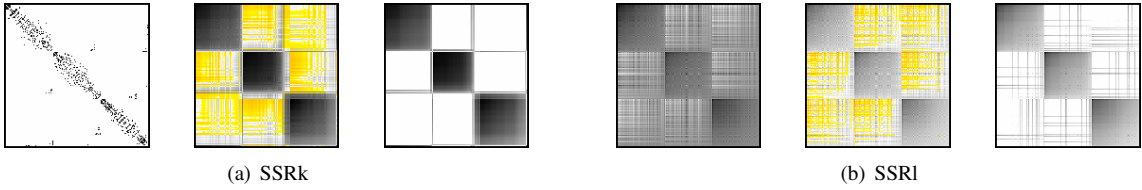


Figure 9: Gram matrices of G2 data. Yellow color indicates negative value (the heavier the color, the smaller the value). In each subfigure, left: similarity matrix/Gram matrix of augmented data, i.e.,  $W$ , middle:  $H^T H$ , right:  $\bar{H}^T \bar{H}$ . The data is rearranged as Figure 5.

does not necessarily be so. In Figure 10 (a)-(c), the condition is deviated more and more for the linear version, as can be expected from the data distributions of these data sets (see Figure 4(b) and Figure 11).

Next, based on the eigengap (Davis-Kahan) theorem of matrix perturbation (see Theorem 7 of [64]), we propose a  $\rho$  value, measuring how well the ideal graph condition is met. The  $\rho$  value of a similarity matrix  $W \in \mathbb{R}^{n \times n}$  for  $1 \leq r < n$  clusters is defined as

$$\rho = (\lambda_{r+1} - \lambda_r) / \lambda_{r+1}, \quad (60)$$

where  $\lambda_i$  is the  $i$ th smallest eigenvalue of the Laplacian matrix. If  $\lambda_{r+1} = 0$ ,  $\rho$  is defined to be 0. It has the following properties:

**Theorem 20.**  $0 \leq \rho \leq 1$ , and  $\rho = 1$  if and only if the ideal graph condition is met exactly.

*Proof.* When the ideal graph condition is met, according to the properties of Laplacian matrix in Section 3.3,  $\lambda_r = 0$  and  $\lambda_{r+1} \neq 0$ , so  $\rho = 1$ . Conversely, if  $\rho = 1$ , then  $\lambda_{r+1} \neq 0$  and  $\lambda_1 = \dots = \lambda_r = 0$ , implying  $r$  connected components exist, so the ideal graph condition is met.  $\square$

When the graph is nearly ideal,  $\rho \approx 1$ . The better the condition is met, the higher the  $\rho$  is. A comparison of the  $\rho$  values between the linear version and kernel version are shown in Table 3. It is clear that generally the kernel version meets the condition better than the linear version.

Finally, the clustering performance are compared in Table 4. The results on TDT2 and polb are absent, since the linear version fails to run on them. The kernel version generally performs better, for it meets the ideal graph condition better. The contrasts are most apparent on onion, iris, and wdbc, as implied by Figure 10. But, the results are reversed on G2 and G3, maybe the linear version meets the condition well (see Figure 10(a)).



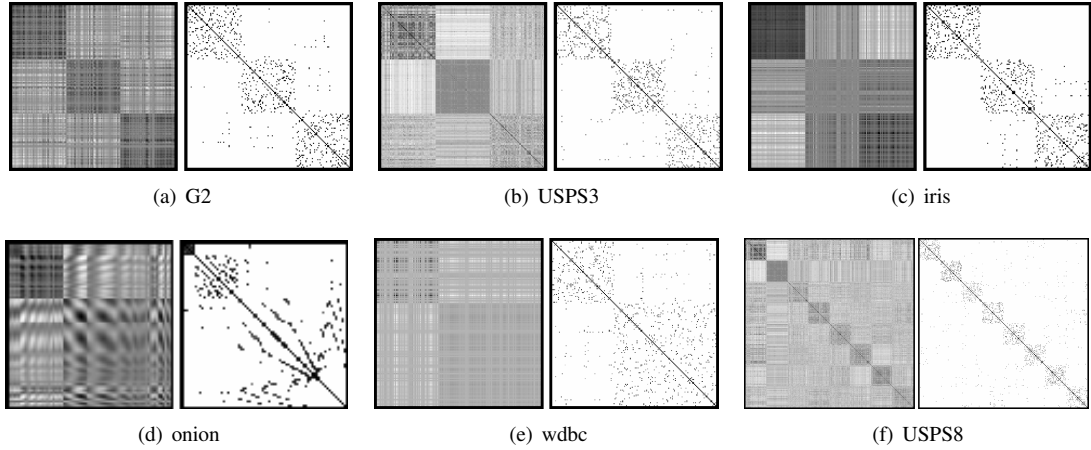


Figure 10: Linear version v.s. kernel version: a comparison of the similarity matrices. In each subfigure, left: linear version, right: kernel version.

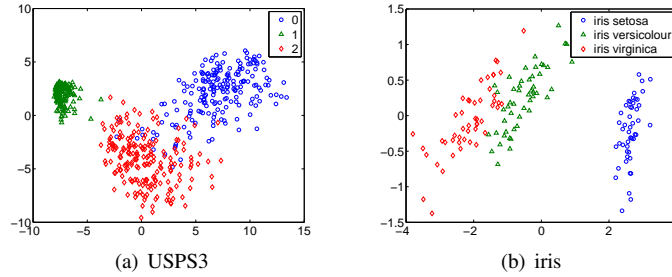


Figure 11: 2D views of USPS3 and iris (the first two PCs of PCA).

## 7.4 Relations between $\rho$ , Sparsity of SSR, and Clustering Accuracy

In principle,  $\rho$  reflects the separability of the clusters, it thus relates to the clustering accuracy. On the other hand, it implies the noise level in the indicator vectors, which is related to the sparsity of codes. Therefore, there are proportional relations between them. We validate the relations by a set of Gaussian data with more and more heavy overlaps (like G1-G3). The result is shown in Figure 12, clear proportional relations can be observed. The relations imply that, potentially, the  $\rho$  value, which can be computed once the data is given, may provide us an estimation of the sparsity and the clustering performance before SSR and  $Scut$  are applied or when the ground-truth class labels are not available.

## 7.5 Clustering via Kernel $Scut$

Since the superiority of kernel version has been demonstrated in previous section, now we focus on kernel  $Scut$  and compare it with some popular algorithms.

The results of accuracy, NMI, and RI are shown in Table 5.<sup>17</sup> According to the mean scores of the three criteria,  $Scut$  performs best overall. Although the scores of  $Rcut$  are comparable to those of  $Scut$ , they are the best ones picked over 20 trials, the mean scores of  $Rcut$  are much worse, and the variances are large, as shown in Table 4. The difference between  $Rcut$  and  $Scut$  is that  $Rcut$  employs Kmeans to recover the indicators, while  $Scut$  employs NSCrT. In view of the comparable results of  $Scut$  to the optimal results of  $Rcut$ , it probably indicates that NSCrT has accurately recovered the underlying indicators. ZP and  $Ncut$  address similar problems too, especially ZP, which tries to recover indicators via rotation as NSCrT does. However, the results show that they do not perform as well

<sup>17</sup>Codes of Graclus and  $Ncut$  are downloaded from <http://www.cs.utexas.edu/users/dml/Software/graclus.html> and <http://www.cis.upenn.edu/~jshi/software/> respectively. GMM and Kmeans are provided by MATLAB toolbox. The remaining methods are implemented by us using MATLAB. GMM cannot run on 4News and TDT2 due to  $p > n$ , and Kmeans fails to run on TDT2.

Table 4: Linear version v.s. kernel version: clustering performance. K-PC: K-means applied on PCs  $\Sigma_{1:r-1}V_{1:r-1}$ . Rcutl: K-means applied on  $V_{1:r-1}$ . Scutl: Scut of SSRI. Rcut and Scut refer to kernel versions by default. For the algorithms that depend on random initialization, mean/standard deviation of the accuracy over 20 trials are reported. The last row shows the mean over all data sets.

Accuracy (%)	Linear version				Kernel version	
	Kmeans	K-PC	Rcutl	Scutl	Rcut	Scut
G1	91.0 / 18.5	93.5 / 15.9	97.6 / 10.6	<b>100.0</b>	91.4 / 17.6	<b>100.0</b>
G2	95.3 / 0.0	95.3 / 0.0	<b>96.0</b> / 0.0	95.3	90.8 / 8.3	92.7
G3	82.7 / 0.0	82.7 / 0.0	82.7 / 0.0	<b>83.3</b>	82.0 / 0.0	82.0
onion	61.7 / 6.9	62.5 / 7.2	62.6 / 5.2	61.3	90.5 / 6.6	<b>90.7</b>
iris	81.5 / 13.9	80.8 / 13.9	77.3 / 0.0	78.0	87.4 / 9.1	<b>95.3</b>
wdbc	85.4 / 0.0	85.4 / 0.0	85.4 / 0.0	87.5	<b>88.9</b> / 0.0	88.4
Isolet	71.7 / 4.9	70.8 / 5.6	71.9 / 4.6	65.0	65.0 / 7.5	<b>82.0</b>
USPS3	92.0 / 0.0	78.3 / 0.0	71.7 / 0.0	72.6	97.2 / 8.6	<b>99.2</b>
USPS8	74.7 / 6.3	74.3 / 3.5	74.2 / 3.8	76.3	74.1 / 10.6	<b>91.0</b>
USPS10	65.6 / 2.8	61.8 / 4.0	65.5 / 1.5	64.9	<b>66.6</b> / 8.8	66.4
4News	88.3 / 10.4	88.7 / 6.7	82.3 / 15.0	94.9	91.8 / 10.0	<b>96.0</b>
Average	80.9 / 5.8	79.5 / 5.2	78.8 / 3.7	79.9	84.2 / 7.9	<b>89.4</b>

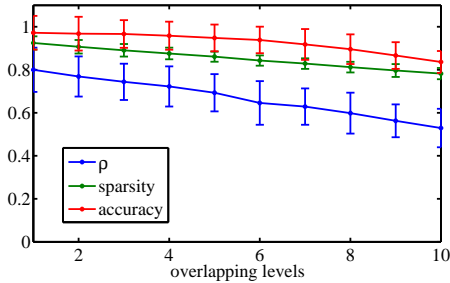


Figure 12: The relations between  $\rho$ , sparsity of SSRk, and clustering accuracy of kernel Scut on a set of random Gaussian data with more and more heavy overlaps. The curve and the bar show the mean and the standard deviation over 50 trials respectively.

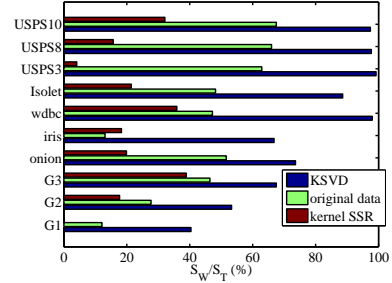


Figure 13: Comparison of the ratios of within-class distance between the original data, sparse codes of KSVd, and sparse codes of SSRk. On G1, the ratio of SSRk is zero.

as Scut. Graclus occasionally does best on some data sets, however, it performs poorly on some well-separable data sets, e.g., onion, iris, and TDT2.

The time cost on the three largest data sets, USPS10, 4News, and TDT2, is shown in Table 6. GMM and Kmeans are much slower. Scut is comparable to the most efficient method, Graclus. Designed to improve the computational cost of traditional spectral clustering methods, Graclus avoids the computation of eigenvectors. However, the total time cost of those methods working with similarity matrix, including Scut and Graclus, is dominated by the construction of similarity matrix. As a consequence, the cost of Scut is still close to that of Graclus. Table 6(b) highlights the cost of the post-processing of eigenvectors. On the largest data set TDT2, Scut is significantly faster than the others, since the time complexity of Scut is  $O(nr^2)$  scaling linearly with data size.

Finally, as popular application of spectral clustering, image segmentation is compared between Rcut, Graclus, Ncut, and Scut. Results on two typical images are shown in Figure 14. The images and their similarity matrices are obtained from the web site of Ncut: <http://www.cis.upenn.edu/~jshi/software/>.

## 7.6 OSRs v.s. SSR on clustering

We compare the two most related OSRs: KSVd and SSC [27], with SSR on clustering. Below, absence of results on 4News and TDT2 are due to running out of memory of KSVd and SSC.

First, for KSVd, we learn a dictionary and codes with the same sizes as SSRI, and apply the same clustering strategy as Scut.<sup>18</sup> The results are shown in Table 7. Scutl outperforms KSVd and SSC significantly. Next, we

<sup>18</sup>The maximal  $\ell_0$ -norm of KSVd is set to be  $\lceil r/3 \rceil$ . Considering KSVd depends on random initialization, it is repeated 20 times, and the

Table 5: Comparison of the clustering results between kernel Scut and Graclus [19], Ncut [73], ZP [75], GMM-V (Gaussian mixture model, applied on  $V_{1:r}$  of Laplacian matrix), GMM (applied on original data), Kmeans, NJW [47], and Rcut. For algorithms that depend on random initialization (from GMM-V to Rcut), the score when the objective function obtains the best value over 20 trials is reported. The last row shows the average score over all data sets.

(a) Accuracy

Accuracy (%)	Graclus	Ncut	ZP	GMM-V	GMM	Kmeans	NJW	Rcut	Scut
G1	<b>100.0</b>	<b>100.0</b>	<b>100.0</b>	<b>100.0</b>	<b>100.0</b>	<b>100.0</b>	<b>100.0</b>	<b>100.0</b>	<b>100.0</b>
G2	92.7	93.3	92.7	93.3	<b>96.0</b>	95.3	92.7	92.7	92.7
G3	<b>84.0</b>	81.3	81.3	81.3	54.7	82.7	81.3	82.0	82.0
onion	62.7	90.7	90.7	73.3	<b>93.3</b>	57.3	90.7	92.0	90.7
iris	87.3	87.3	88.0	84.0	52.7	89.3	90.0	90.0	<b>95.3</b>
wdbc	88.4	77.7	88.2	83.5	85.1	85.4	81.9	<b>88.9</b>	88.4
Isolet1	76.8	80.9	70.7	73.5	55.6	81.4	80.5	<b>82.2</b>	82.0
USPS3	<b>99.5</b>	60.9	99.2	99.2	95.7	92.0	99.2	99.1	99.2
USPS8	80.2	47.9	92.1	85.7	67.8	72.2	90.8	<b>93.3</b>	91.0
USPS10	<b>78.9</b>	67.3	64.6	75.8	49.4	67.8	66.5	66.8	66.4
4News	95.6	<b>96.1</b>	95.7	71.3	-	92.2	<b>96.1</b>	95.8	96.0
TDT2	54.4	88.0	84.4	71.6	-	-	70.7	76.6	<b>88.5</b>
polb	83.8	82.9	84.8	81.0	-	-	82.9	<b>87.6</b>	84.8
Average	83.4	81.1	87.1	82.6	75.0	83.2	86.4	88.2	<b>89.0</b>

(b) NMI

NMI (%)	Graclus	Ncut	ZP	GMM-V	GMM	Kmeans	NJW	Rcut	Scut
G1	<b>100.0</b>	<b>100.0</b>	<b>100.0</b>	<b>100.0</b>	<b>100.0</b>	<b>100.0</b>	<b>100.0</b>	<b>100.0</b>	<b>100.0</b>
G2	76.4	78.5	75.5	78.5	<b>83.9</b>	80.9	75.5	75.5	75.5
G3	<b>56.9</b>	49.4	49.4	49.6	26.2	48.6	49.4	50.8	50.4
onion	44.6	68.4	68.4	37.9	<b>74.4</b>	46.4	68.4	71.4	68.4
iris	75.0	75.0	75.6	72.2	65.4	75.8	77.8	77.8	<b>84.6</b>
wdbc	49.4	35.2	49.0	42.5	37.1	46.7	39.2	<b>49.9</b>	49.4
Isolet1	79.8	88.0	82.0	83.6	62.7	84.8	87.8	87.6	<b>88.2</b>
USPS3	<b>97.2</b>	58.5	95.8	95.7	84.6	80.0	95.8	95.4	95.8
USPS8	85.8	66.9	86.8	83.7	55.7	70.5	85.6	<b>87.2</b>	86.2
USPS10	<b>81.0</b>	80.1	77.6	79.0	41.0	64.0	78.6	78.8	78.4
4News	84.3	<b>85.7</b>	84.2	65.1	-	81.4	<b>85.7</b>	84.8	85.4
TDT2	74.2	<b>85.5</b>	83.1	76.1	-	-	80.8	83.5	85.0
polb	55.4	54.2	58.6	57.8	-	-	54.2	<b>65.1</b>	58.6
Average	73.8	71.2	75.8	70.9	63.1	70.8	75.3	<b>77.5</b>	77.4

(c) RI

RI (%)	Graclus	Ncut	ZP	GMM-V	GMM	Kmeans	NJW	Rcut	Scut
G1	<b>100.0</b>	<b>100.0</b>	<b>100.0</b>	<b>100.0</b>	<b>100.0</b>	<b>100.0</b>	<b>100.0</b>	<b>100.0</b>	<b>100.0</b>
G2	90.8	91.6	90.8	91.6	<b>94.8</b>	94.0	90.8	90.8	90.8
G3	<b>81.7</b>	79.0	79.0	78.6	56.7	79.7	79.0	79.2	79.6
onion	66.7	85.3	85.3	63.8	<b>88.7</b>	64.1	85.3	86.5	85.3
iris	86.2	86.2	86.8	83.7	72.2	88.0	88.6	88.6	<b>94.2</b>
wdbc	79.5	65.3	79.2	72.4	74.5	75.0	70.3	<b>80.3</b>	79.5
Isolet1	96.7	<b>97.5</b>	95.6	96.2	93.1	97.3	97.4	97.2	<b>97.5</b>
USPS3	<b>99.4</b>	73.9	99.0	98.9	95.0	90.8	99.0	98.9	99.0
USPS8	94.6	83.1	96.4	95.7	88.1	91.5	96.2	<b>96.8</b>	96.0
USPS10	<b>94.6</b>	93.5	92.9	<b>94.6</b>	78.8	91.7	93.3	93.2	93.2
4News	95.7	<b>96.3</b>	95.8	83.6	-	92.5	<b>96.2</b>	95.9	96.1
TDT2	91.3	<b>96.3</b>	95.3	93.7	-	-	93.8	95.1	96.2
polb	83.6	83.1	85.0	81.4	-	-	83.1	<b>86.6</b>	85.0
Average	82.4	87.0	90.9	87.2	84.2	87.7	90.2	91.5	<b>91.7</b>

Table 6: Time cost on the three largest data sets, USPS10 (256×7291, 10 classes), 4News (26214×2372, 4 classes), and TDT2 (36771×9394, 30 classes). The total time cost includes the construction of similarity matrix, computation of eigenvectors, and post-processing of eigenvectors.

(a) Total time cost

Time (s)	Graclus	Neut	ZP	GMM-V	GMM	Kmeans	NJW	Rcut	Scut
USPS10	<b>7.5</b>	8.2	12.0	11.0	101.0	8.7	7.9	7.9	8.0
4News	<b>1.1</b>	1.1	1.5	1.5	-	584.7	1.1	1.4	1.5
TDT2	<b>17.7</b>	19.7	187.8	47.1	-	-	22.8	22.7	19.3

(b) Time cost of post-processing eigenvectors

Time (s)	ZP	GMM-V	NJW	Rcut	Scut
USPS10	4.20	3.13	<b>0.08</b>	0.10	0.12
4News	0.05	0.06	<b>0.01</b>	0.01	0.05
TDT2	168.80	28.10	2.66	3.69	<b>0.34</b>

Table 7: KSVD and SSC v.s. SSRI on clustering. KSVD has the same size of dictionary and codes as SSRI, and non-maximum suppression is applied for clustering. The mean accuracy of KSVD over 20 trials is shown.

Accuracy (%)	G1	G2	G3	onion	iris	wdbc	Isolet	USPS3	USPS8	USPS10
KSVD	95.9	86.0	67.5	64.7	62.6	66.5	56.3	67.9	57.2	49.2
SSC	<b>100.0</b>	66.7	53.3	60.0	<b>78.0</b>	87.3	<b>78.8</b>	59.0	-	-
Scutl	<b>100.0</b>	<b>95.3</b>	<b>83.3</b>	<b>61.3</b>	<b>78.0</b>	<b>87.5</b>	65.0	<b>72.6</b>	<b>76.3</b>	<b>64.9</b>

learn an over-complete KSVD and apply K-means on the codes.<sup>19</sup> Comparing with kernel Scut, the clustering results are shown in Table 8. Scut still performs better.

To investigate the reason of the inferior performance of KSVD against SSR, we compare how well the cluster structure of data is enhanced by the two kinds of sparse codes. This is measured by the ratio of within-class distance,  $S_W/S_T = \sum_{k=1}^K \sum_{H_i \in C_k} \|H_i - D_k\|_2^2 / \sum_{j=1}^n \|H_j - d\|_2^2$ , where  $D_k$  is the mean of class  $C_k$ , and  $d$  is the mean of the whole set. The ratio is between 0 and 1. Smaller value implies better separability. In the same setting as last experiment, the ratios are shown in Figure 13. We see that the ratios of SSR are generally smaller than those of original data, which means SSR enhances the cluster structure. However, those of KSVD are significantly larger, implying the codes of KSVD are dispersed, which may not suitable for clustering purpose.

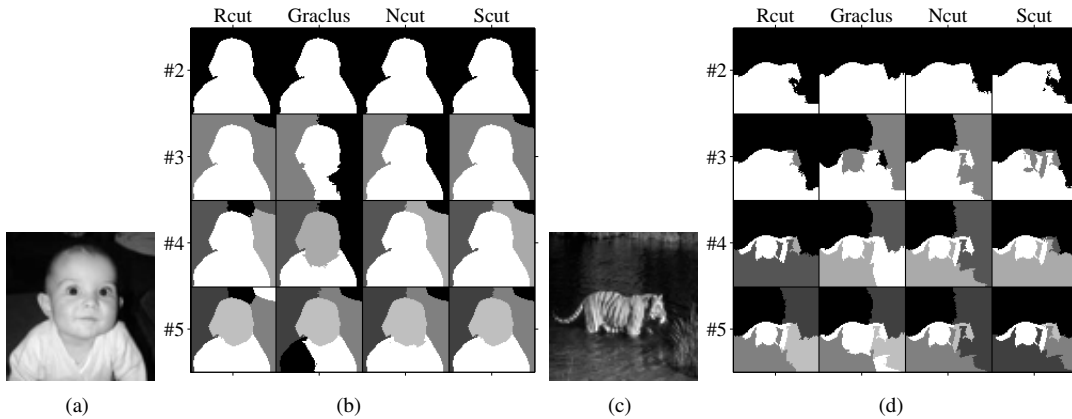


Figure 14: Examples of image segmentation results. (a), (c) Original 80 × 80 gray images. (b), (d) Segmentation results. The rows correspond to number of clusters.

mean accuracy is reported, since there is no suitable criterion to pick the optimal result. Codes of SSC is the ADMM version downloaded from <http://www.cis.jhu.edu/~ehsan/code.htm>. Independent affine subspaces is assumed for better performance.

<sup>19</sup>The number of atoms and the maximal  $\ell_0$ -norm are set to be  $m = \min(2p, \lceil n/5 \rceil)$  and  $\min(8, \lceil m/3 \rceil)$  respectively.

Table 8: KSVD+Kmeans v.s. kernel Scut. For KSVD, the optimal accuracy with respect to objective function of Kmeans over 20 trials is shown.

Accuracy (%)	G1	G2	G3	onion	iris	wdbc	Isolet	USPS3	USPS8	USPS10
KSVD	91.3	<b>93.3</b>	74.7	58.7	82.0	67.0	23.9	43.1	19.7	17.5
Scut	<b>100.0</b>	92.7	<b>82.0</b>	<b>90.7</b>	<b>95.3</b>	<b>88.4</b>	<b>82.0</b>	<b>99.2</b>	<b>91.0</b>	<b>66.4</b>

## 8 Extended Relations to Other Methods

We have established the inherent relations between PCA/LE, K-means/Rcut, and SSR so far. In this section, we will further link the framework to OSRs, kernel PCA, manifold learning, and subspace clustering.

### 8.1 Relation between OSRs and SSRI

We focus on two classical OSRs: [49] and KSVD [2], and compare them with SSRI. The relation will be explored mainly from the row-space view, rather than the column-space view that is sample-wise. It will be shown that the commonality of the methods is to find a sparse basis that covers the row space of data as much as possible. The sparse basis consists of the row vectors of the code matrix. The basis size can be chosen differently, whose range lies in  $[0, n]$ . OSRs and SSRI occupy different sections of the range, that is where the difference comes from, and it leads to distinct solution strategies.

The objectives of [49] and KSVD are

$$\min_{D \in \mathbb{R}^{p \times r}, X \in \mathbb{R}^{r \times n}} \|A - DX\|_F^2 + \lambda \|X_i\|_1, i = 1, \dots, n, \quad (61)$$

$$\min_{D \in \mathbb{R}^{p \times r}, X \in \mathbb{R}^{r \times n}} \|A - DX\|_F^2, \text{ s. t. } \|X_i\|_0 \leq L, i = 1, \dots, n, \quad (62)$$

respectively, where,  $p < r \leq n$ , i.e., over-complete. We assume in this discussion  $\text{rank}(A) = p$ .

Due to implicit sparsity constraint, the objective of SSRI can be expressed as

$$\min_{D \in \mathbb{R}^{p \times r}, X \in \mathbb{R}^{r \times n}} \|A - DX\|_F^2, \text{ s. t. } XX^T = I, X \text{ sparse}, \quad (63)$$

where  $r \leq p + 1$ , i.e., usually under-complete.

Fixing  $X$ ,  $D^* = AX^T(XX^T)^{-1}$ . Substituting it into the objectives, all of them reduce to

$$\min_X \|A - AX^T(XX^T)^{-1}X\|_F^2, \text{ s. t. } X \text{ sparse}, \quad (64)$$

with various sparse constraints on  $X$ . Since  $X^T(XX^T)^{-1}X$  is a projection matrix formed by the row vectors of  $X$ , the above objective can be interpreted as: to find a sparse basis so that it covers the row space of data as much as possible. This is the common point of the three SRs.

The sparse basis of SSRI is obtained via rotating the normalized PCs (attached with  $\mathbf{1}^T/\sqrt{n}$ ), showing a close tie to PCA. SSRI is also related to cluster analysis, due to the one-one correspondence between the normalized PCs and the eigenvectors of a linear Laplacian matrix. The basis size of SSRI is limited by the number of PCs, or equivalently the effective eigenvectors of Laplacian matrix. The over-completeness prevents OSRs from the reach of spectral graph theory as well as PCA, when  $r > p + 1$ . We do not know which vectors to draw from the void subspace that is complementary to the data row-space, so that attaching to the PCs and via rotation, they turn into sparse basis.

The dilemma is circumvented by resorting to the dictionary representation. Treating the dictionary and codes independently, OSRs obtain solution by alternate optimization. This strategy depends on a random initialization of the dictionary, which can be seen as replacing drawing vectors from the complementary row-subspace. The initialization is usually done via randomly drawing samples from the data set. Expressing  $D = AX^T(XX^T)^{-1}$ , it is still not clear what the corresponding sparse codes are. However, if the dictionary is initialized with cluster centers, e.g., of K-means, the sparse codes are obviously the corresponding indicator vectors. Then following the

alternate optimization,  $D$  is fixed, the extreme sparse codes are relaxed and updated to soft ones, via some sample-wise sparse coding algorithms, e.g., OMP [50], BP [12], and then  $D$  is updated and so on.<sup>20</sup> Notice that, K-means itself belongs to the SSR framework, while its solution adopts the alternate optimization. Unlike Rcut, K-means can obtain clusters more than the number of PCs. The cluster centers of K-means are usually initialized with random samples. Combining the two solution processes together, the above strategy is in fact K-means+OSR,<sup>21</sup> in hindsight, it is interesting to find their counterpart PCA+SSR. At this point, the close ties between these methods are clear. A diagram is illustrated in Figure 1.

Further more, the four methods can be eventually unified at an extreme point,  $r = n$ . At  $r = n$  there is no choice, the whole complementary subspace has been included. A rotation of the full basis can lead to the ultimate sparse basis: the identity matrix. In this case, the dictionary consists of the whole data sets, with each sample serving as an atom/cluster center. They must be the optimal solution of OSRs and K-means too. This seemingly useless extreme sparse representation had found its application in face recognition [69].

Finally, we comment that attributing to the random initialization, the formal relation of OSRs to cluster analysis is less obvious than that of SSRI, except a special case of KSVD; and the clustering performance of KSVD is not satisfactory as the experiments demonstrated. Nevertheless, the basis size SSRI can handle is limited, and OSRs had demonstrated impressive performance on signal denoising and reconstruction [25]. As sparse representation methods, SSRI and OSRs occupy different ranges and complement each other.

## 8.2 Relations between Kernel PCA, Manifold Learning, and SSR

First, we will show that kernel PCA (KPCA) [57] can be incorporated into the framework of SSR. The underlying reason is simple: PCA constitutes a part of SSR framework, and KPCA can be seen as a PCA, with original data replaced by high-dimensional features. Next, the relation is extended to manifold learning, including multidimensional scaling (MDS) [16], Isomap [62], and locally linear embedding (LLE) [53].

Let  $G$  be a kernel matrix, and assume to find normalized PCs, the objective of KPCA is

$$\max_X \text{tr}\{X(I - \frac{1}{n}\mathbf{1}\mathbf{1}^T)G(I - \frac{1}{n}\mathbf{1}\mathbf{1}^T)X^T\}, \text{ s. t. } XX^T = I.$$

Then we have

**Theorem 21.** *There is a sparse representation of KPCA:  $\begin{bmatrix} \frac{1}{\sqrt{n}}\mathbf{1}^T \\ V_{1:r-1} \end{bmatrix} = RH$ , where  $V_{1:r-1}$  are the eigenvectors of KPCA.*

*Proof.* Assume LE uses the same kernel matrix, and the original data  $A$  is not mean-removed, then PCA, KPCA, and LE can be seen as working with the following three similarity matrices respectively:  $W_{PCA} = \beta\mathbf{1}\mathbf{1}^T + \bar{A}^T\bar{A}$ ,  $W_{KPCA} = \beta'\mathbf{1}\mathbf{1}^T + G_{KPCA}$ , and  $W_{LE} = G$ , where  $\bar{A} = A(I - \frac{1}{n}\mathbf{1}\mathbf{1}^T)$ ,  $G_{KPCA} = (I - \frac{1}{n}\mathbf{1}\mathbf{1}^T)G(I - \frac{1}{n}\mathbf{1}\mathbf{1}^T)$ , and  $\beta, \beta'$  ensure the nonnegativity of the corresponding similarity matrices. The solution of PCA is obtained from the eigenvectors of  $\bar{A}^T\bar{A}$ , while that of KPCA is obtained from the eigenvectors of  $G_{KPCA}$ . By the correspondence between  $\bar{A}^T\bar{A}$  and  $G_{KPCA}$ , following the conversion from PCA to SSRI, the assertion is established.  $\square$

It implies KPCA is inherently related to cluster analysis too. We may wonder to what extent does KPCA reveal cluster structure, and how the clustering performance will be when using Scut. These questions can be answered by the ideal graph condition. Following the analysis of SSRI, we expect the similarity matrix used by KPCA meets the condition better than that used by PCA while worse than that used by LE. Though not reported, our experiments validated this. Besides, we mention that a significant drawback of KPCA is that it demands a large storage when dealing with large data sets, due to the dense kernel matrix.

Once KPCA has joined the SSR framework, a series of manifold learning [33] or graph embedding [70] methods, including MDS, Isomap, and LLE, subsequently share extended relations to SSR. It is because, under a kernel view, these methods can be written into the form of KPCA, as is well-known in the literature [33, 6, 70]. In particular, it had been proven that classical MDS using Euclidean distance is exactly equivalent to PCA [67]. For

<sup>20</sup>In KSVD, when the maximal  $\ell_0$ -norm of codes is constrained to 1, KSVD reduces to vector quantization [32], and if further the nonzero value is constrained to be 1, it reduces to exactly K-means, as [2] had analyzed. The reverse process generalizes K-means to KSVD [2].

<sup>21</sup>Similar strategies of clustering+OSR have been used in the proofs of exact dictionary recovery [1], showing some underlying relation between OSR and cluster analysis.

metric MDS, Isomap (a special metric MDS that uses geodesic manifold distances), and LLE, relations to KPCA exist, although less rigorous, due to the kernel functions of their constructed “kernel matrices” are ambiguous [33].

Finally, it should be clarified that when we talk about the relations, it does not mean that dimensionality reduction or manifold learning is always related to SSR or cluster analysis. When the data do not exhibit cluster structure, these methods work as usual, and the codes preserve the data proximity. When clusters emerge in the data distribution, noisy or not, the codes are intrinsically embedded with cluster structure. Depending on two things, the structure becomes explicit: the attachment of vector  $\mathbf{1}$  and a proper rotation. We believe that for most real-world data, some underlying clusters naturally exist, more or less, and in a hierarchical way. Therefore, the codes must generally contain some cluster information, and the link of dimensionality reduction or manifold learning methods to SSR and cluster analysis should be commonplace. This explains why in so many paper focusing on manifold learning, the codes, when reduced to two dimensions for visualization, frequently exhibit a triangle shape (three clusters, cf. Figure 8). Plenty of examples can be found, e.g., in [55, 60, 56].

### 8.3 Relations between Subspace Clustering, LLE, and SSRI

A series of work in subspace clustering, represented by SSC [27], low-rank representation (LRR) [40], and the manifold learning method LLE [53] center around the seemingly trivial data representation form  $A \approx AZ$ , which has been repeatedly interpreted in PCA, K-means, and SSR. We will show that SSC, LRR, LLE, and SSRI are related to each other, and the ideal graph condition is a special case of the ideal working condition of subspace clustering.

In cluster analysis, besides the clusters formed by spatial proximity, there is another circumstance that the clusters are formed by a union of linear subspaces, with one subspace corresponding to one cluster. The latter case is the subject of subspace clustering [63], which has found applications in, e.g., motion and image segmentation, face recognition [27, 40]. SSRI/Scutl may belong to this domain too. The ideal graph condition of linear version requires that the clusters should be orthogonal.<sup>22</sup> This is a special case of the ideal working condition of subspace clustering, i.e., the subspaces being linearly independent.

The first step of SSC, LRR, LLE, and SSRI can be viewed as finding some code matrix to represent the data matrix with respect to a dictionary composed of the data matrix itself, i.e., solving  $\|A - AZ\|_F^2$  with some constraint on  $Z$ . The problem is generally under-determined, with infinitely many solutions achieving zero error, e.g., the identity matrix and the Gram matrix  $V^T V$ , where  $V$  is the full normalized PCs of data. SSC finds a sparse solution with the constraint that the diagonal being zero, i.e., forbidding self-representation. LRR finds a low-rank solution via minimizing the nuclear norm of  $Z$ , which turned out to be  $V^T V$  uniquely. LLE finds a sparse solution such that the nonzero entries of each column are constrained to the neighborhood of the associated point, and they sum to 1, i.e., each point is approximated locally by its neighborhood. For SSRI, we have  $A \approx A(H^T H)$ . Note  $H^T H = V_{1:r}^T V_{1:r}$ , which is the Gram matrix of  $r$  PCs. SSC and LRR can achieve zero reconstruction error while SSRI is optimal within rank- $r$  limitation.

In the second step, SSC, LRR, and SSRI aim at clustering, while LLE is oriented to dimensionality reduction. When the subspaces are independent, [27] (excluding minor factors) and [40] proved their solutions are block-diagonal, if the data are arranged orderly. That is each point can be exactly reconstructed by its subspace. When the subspaces are orthogonal as the ideal graph condition requires, it is easy to see that all code matrices of the four methods become block-diagonal. Block-diagonal property is desirable, since it suits for the clustering purpose. In the second step of SSC and LRR, a similarity matrix is heuristically built based on  $Z$ , e.g.,  $W = |Z| + |Z|^T$  in SSC, then spectral clustering is employed to finish clustering. Since the code matrices are block-diagonal, so are the similarity matrices. It implies an ideal graph condition of kernel version is satisfied, making spectral clustering easy. For SSRI, this step can be omitted and clustering can be done by applying Scutl on  $H$ , since the code matrix  $H^T H$  itself is a qualified similarity matrix, and the eigenvectors of the associated Laplacian matrix is exactly  $H$ . In the second step of LLE, it seeks low-dimensional codes  $X \in \mathbb{R}^{r \times n}$ , such that it replaces original data and the neighborhood structure of data is preserved:  $\min_X \|X - XZ\|_F^2$ , s.t.  $XX^T = I$ . For SSRI, this step can be omitted too, since  $H$  itself is the codes and also the solution of LLE’s objective when  $Z = H^T H$ .

Although LLE is designed for dimensionality reduction, by the same principle of SSC and LRR, it can be used for clustering too. Conversely, following LLE, SSC and LRR can be used for dimensionality reduction, regardless of the clusters. But only SSRI covers both domains in a natural way. We again witness the ambiguous borders between dimensionality reduction, sparse representation, and cluster analysis.

<sup>22</sup>In this section, for SSRI, we consider the augmented data. For SSC and LRR, we focus on their basic models.

## 9 Conclusion and Future Work

In this paper, we have established a spectral graph-based framework unifying dimensionality reduction, cluster analysis, and sparse representation. It includes the inherent relations between PCA, K-means, LE, Rcut, SSR, and extended relations to OSRs, manifold learning, and subspace clustering. Based on the unification of PCA, K-means, LE, Rcut, a new sparse representation, SSR, has been derived. An efficient algorithm, NSCrT, has been developed to solve the sparse codes of SSR. As an application of SSR, the new clustering algorithm Scut achieved the state-of-the-art performance in the spectral clustering family.

The future work may include as follows. First, the theoretical analysis of whether NSCrT has the ability to recover underlying solution remains an open question. It is essentially a dictionary recovery problem. Recent results have shed light on it, e.g., [61, 1, 3]. Especially, [61] deals with square dictionary, and they proved that in noise-free case the dictionary can be recovered with high probability when each column of the codes has at most  $O(\sqrt{r})$  nonzeros and there are at least  $\Omega(r^2 \log^2 r)$  samples. It matches our case closely. Second, this paper remains in the unsupervised learning domain. It is interesting to find out whether the supervised classification can be incorporated into the spectral graph framework. Finally, in view of the relations of SSR to many other methods, as well as the nice properties it has, we envision that SSR may have other potential applications, especially the out-of-sample case.

## A An Interpretation for Kernel Scut

In SSRk, Scut can be interpreted as clustering data according to the smallest included angle (or distance) between the cluster centers and the virtual data. By Theorem 14, the atoms of  $\hat{D}$  are cluster centers that are near-orthogonal and have similar lengths. In this case, it can be proved that

$$\begin{aligned}
& \arg \max_k \cos(\theta(\hat{D}_k, \tilde{A}_i)) \\
&= \arg \max_k \hat{D}_k^T \tilde{A}_i / (\|\hat{D}_k\|_2 \cdot \|\tilde{A}_i\|_2) \\
&\approx \arg \max_k \hat{D}_k^T \tilde{A}_i && (\text{since } \|\hat{D}_k\|_2 \approx \lambda_n^{\frac{1}{2}}) \\
&\approx \arg \max_k [\lambda_n^{\frac{1}{2}} R_k^T, \mathbf{0}] (\lambda_n I - \Lambda)^{\frac{1}{2}} V_i && (\text{by (39) and definition of } \tilde{A}) \\
&= \arg \max_k \lambda_n^{\frac{1}{2}} R_k^T (\lambda_n I - \Lambda_{1:r})^{\frac{1}{2}} (V_{1:r})_i \\
&\approx \arg \max_k \lambda_n R_k^T R H_i && (\text{by } \Lambda_{1:r} \approx \mathbf{0} \text{ and } V_{1:r} = R H) \\
&= \arg \max_k H_{ki},
\end{aligned} \tag{65}$$

which implies Scut performs clustering based on the smallest included angle.

Besides, since  $\arg \min_k \|\tilde{A}_i - \hat{D}_k\|_2^2 = \|\tilde{A}_i\|_2^2 + \|\hat{D}_k\|_2^2 - 2\hat{D}_k^T \tilde{A}_i \approx \arg \max_k \hat{D}_k^T \tilde{A}_i$ , Scut can also be interpreted as clustering data according to the smallest distance to the cluster centers.

## References

- [1] Alekh Agarwal, Animashree Anandkumar, and Praneeth Netrapalli. Exact recovery of sparsely used overcomplete dictionaries. *Arxiv*, 2013.
- [2] Michal Aharon, Michael Elad, and Alfred Bruckstein. K-SVD: An algorithm for designing overcomplete dictionaries for sparse representation. *IEEE Transactions on Signal Processing*, 54(11):4311–4322, 2006.
- [3] Sanjeev Arora, Rong Ge, and Ankur Moitra. New algorithms for learning incoherent and overcomplete dictionaries. In *Conference on Learning Theory*, volume 35, pages 779–806, 2014.
- [4] Mikhail Belkin and Partha Niyogi. Laplacian eigenmaps for dimensionality reduction and data representation. *Neural Computation*, 15(6):1373–1396, 2003.



- [5] Yoshua Bengio, Olivier Delalleau, Nicolas Le Roux, Jean-François Paiement, Pascal Vincent, and Marie Ouimet. Learning eigenfunctions links spectral embedding and kernel PCA. *Neural Computation*, 16(10):2197–2219, 2004.
- [6] Yoshua Bengio, Jean-François Paiement, Pascal Vincent, Olivier Delalleau, Nicolas Le Roux, and Marie Ouimet. Out-of-sample extensions for lle, isomap, mds, eigenmaps, and spectral clustering. In *Advances in Neural Information Processing Systems*, volume 16, page 177. MIT Press, 2004.
- [7] Christopher M Bishop. *Pattern Recognition and Machine Learning*. Springer New York, 2006.
- [8] Y-Lan Boureau, Francis Bach, Yann LeCun, and Jean Ponce. Learning mid-level features for recognition. In *IEEE Conference on Computer Vision and Pattern Recognition*, pages 2559–2566. IEEE, 2010.
- [9] Alfred M Bruckstein, David L Donoho, and Michael Elad. From sparse solutions of systems of equations to sparse modeling of signals and images. *SIAM Review*, 51(1):34–81, 2009.
- [10] Emmanuel J Candès and Michael B Wakin. An introduction to compressive sampling. *IEEE Signal Processing Magazine*, 25(2):21–30, 2008.
- [11] Pak K Chan, Martine DF Schlag, and Jason Y Zien. Spectral k-way ratio-cut partitioning and clustering. *IEEE Transactions on Computer-Aided Design of Integrated Circuits and Systems*, 13(9):1088–1096, 1994.
- [12] Scott Shaobing Chen, David L Donoho, and Michael A Saunders. Atomic decomposition by basis pursuit. *SIAM Journal on Scientific Computing*, 20(1):33–61, 1998.
- [13] Fan RK Chung. *Spectral Graph Theory*. American Mathematical Society, 1997.
- [14] Adam Coates and Andrew Y Ng. The importance of encoding versus training with sparse coding and vector quantization. In *International Conference on Machine Learning*, pages 921–928. ACM, 2011.
- [15] Michael B. Cohen, Sam Elder, Cameron Musco, Christopher Musco, and Madalina Persu. Dimensionality reduction for k-means clustering and low rank approximation. In *Annual ACM on Symposium on Theory of Computing*, pages 163–172, 2015.
- [16] Trevor F Cox and Michael AA Cox. *Multidimensional scaling*. Chapman and Hall, 2001.
- [17] Fernando De la Torre. A least-squares framework for component analysis. *IEEE Transactions on Pattern Analysis and Machine Intelligence*, 34(6):1041–1055, 2012.
- [18] Inderjit Dhillon, Yuqiang Guan, and Brian Kulis. A unified view of kernel k-means, spectral clustering and graph cuts. *Technical Report No. UTCS TR-04-25*, 2005.
- [19] Inderjit S Dhillon, Yuqiang Guan, and Brian Kulis. Weighted graph cuts without eigenvectors a multilevel approach. *IEEE Transactions on Pattern Analysis and Machine Intelligence*, 29(11):1944–1957, 2007.
- [20] Chris Ding and Xiaofeng He. K-means clustering via principal component analysis. In *International Conference on Machine Learning*, page 29. ACM, 2004.
- [21] Chris HQ Ding, Xiaofeng He, and Hongyuan Zha. A spectral method to separate disconnected and nearly-disconnected web graph components. In *International Conference on Knowledge Discovery and Data Mining*, pages 275–280. ACM, 2001.
- [22] Weisheng Dong, Xin Li, Lei Zhang, and Guangming Shi. Sparsity-based image denoising via dictionary learning and structural clustering. In *IEEE Conference on Computer Vision and Pattern Recognition*, pages 457–464, 2011.
- [23] David Leigh Donoho. Compressed sensing. *IEEE Transactions on Information Theory*, 52(4):1289–1306, 2006.
- [24] Carl Eckart and Gale Young. The approximation of one matrix by another of lower rank. *Psychometrika*, 1(3):211–218, 1936.

- [25] Michael Elad, Mario AT Figueiredo, and Yi Ma. On the role of sparse and redundant representations in image processing. *Proceedings of the IEEE*, 98(6):972–982, 2010.
- [26] Michael Elad, Peyman Milanfar, and Ron Rubinstein. Analysis versus synthesis in signal priors. *Inverse Problems*, 23(3):1–5, 2007.
- [27] Ehsan Elhamifar and Rene Vidal. Sparse subspace clustering: Algorithm, theory, and applications. *IEEE Transactions on Pattern Analysis and Machine Intelligence*, 35(11):2765–2781, 2013.
- [28] K. Engan, S. O. Aase, and J. Hakon Husoy. Method of optimal directions for frame design. In *IEEE International Conference on Acoustics, Speech, and Signal Processing*, volume 5, pages 2443–2446, 1999.
- [29] Martin Ester, Hans-Peter Kriegel, Jörg Sander, and Xiaowei Xu. A density-based algorithm for discovering clusters in large spatial databases with noise. In *International Conference on Knowledge Discovery and Data Mining*, volume 96, pages 226–231. AAAI Press, 1996.
- [30] Ky Fan. A generalization of tychonoff’s fixed point theorem. *Mathematische Annalen*, 142(3):305–310, 1961.
- [31] Shenghua Gao, Ivor Wai-Hung Tsang, and Liang-Tien Chia. Kernel sparse representation for image classification and face recognition. In *European Conference on Computer Vision*, pages 1–14. 2010.
- [32] Allen Gersho and Robert M. Gray. Vector quantization and signal compression. *Springer*, 159(1):407–485, 1992.
- [33] Jihun Ham, Daniel D. Lee, Sebastian Mika, and Bernhard Schölkopf. A kernel view of the dimensionality reduction of manifolds. In *International Conference on Machine Learning*, page 47, 2004.
- [34] Trevor Hastie, Robert Tibshirani, Jerome Friedman, and James Franklin. The elements of statistical learning: data mining, inference and prediction. *The Mathematical Intelligencer*, 27(2):83–85, 2005.
- [35] Xiaofei He and Partha Niyogi. Locality preserving projections. In *Advances in Neural Information Processing Systems*, volume 16, page 153. MIT Press, 2004.
- [36] Zhenfang Hu, Gang Pan, Yueming Wang, and Zhaohui Wu. Sparse principal component analysis via rotation and truncation. *IEEE Transactions on Neural Networks and Learning Systems*, 27(4):875–890, 2016.
- [37] IT Jolliffe. *Principal Component Analysis*. Springer, 2002.
- [38] Harold W Kuhn. The Hungarian method for the assignment problem. *Naval Research Logistics Quarterly*, 2(1-2):83–97, 1955.
- [39] Daniel D Lee and H Sebastian Seung. Learning the parts of objects by non-negative matrix factorization. *Nature*, 401(6755):788–791, 1999.
- [40] Guangcan Liu, Zhouchen Lin, Shuicheng Yan, Ju Sun, Yong Yu, and Yi Ma. Robust recovery of subspace structures by low-rank representation. *IEEE Transactions on Pattern Analysis and Machine Intelligence*, 35(1):171–184, 2013.
- [41] Jun Liu, Shuiwang Ji, and Jieping Ye. *SLEP: Sparse Learning with Efficient Projections*. Arizona State University, 2009.
- [42] James MacQueen. Some methods for classification and analysis of multivariate observations. In *Proceedings of the Fifth Berkeley Symposium on Mathematical Statistics and Probability*, pages 281–297, 1967.
- [43] Christopher D Manning, Prabhakar Raghavan, and Hinrich Schütze. *Introduction to information retrieval*, volume 1. Cambridge University Press, 2008.
- [44] Bojan Mohar. *Some applications of Laplace eigenvalues of graphs*. Springer, 1997.
- [45] Bojan Mohar and Y Alavi. The Laplacian spectrum of graphs. *Graph theory, Combinatorics, and Applications*, 2:871–898, 1991.

- [46] S. Nam, M. E. Davies, M. Elad, and R. Gribonval. The cospase analysis model and algorithms. *Applied and Computational Harmonic Analysis*, 34(1):30–56, 2013.
- [47] Andrew Y Ng, Michael I Jordan, and Yair Weiss. On spectral clustering: analysis and an algorithm. *Advances in Neural Information Processing Systems*, 2:849–856, 2002.
- [48] Feiping Nie, Zinan Zeng, Ivor W Tsang, Dong Xu, and Changshui Zhang. Spectral embedded clustering: a framework for in-sample and out-of-sample spectral clustering. *IEEE Transactions on Neural Networks*, 22(11):1796–1808, 2011.
- [49] Bruno A. Olshausen and David J. Field. Emergence of simple-cell receptive field properties by learning a sparse code for natural images. *Nature*, 381(6583):607–609, 1996.
- [50] Yagyensh Chandra Pati, Ramin Rezaifar, and PS Krishnaprasad. Orthogonal matching pursuit: Recursive function approximation with applications to wavelet decomposition. In *Proceedings of the 27 th Annual Asilomar Conference on Signals, Systems, and Computers*, pages 40–44. IEEE, 1993.
- [51] Ignacio Ramirez, Pablo Sprechmann, and Guillermo Sapiro. Classification and clustering via dictionary learning with structured incoherence and shared features. In *IEEE Conference on Computer Vision and Pattern Recognition*, pages 3501–3508. IEEE, 2010.
- [52] S. Ravishankar and Y. Bresler. Learning sparsifying transforms. *IEEE Transactions on Signal Processing*, 61(5):1072–1086, 2013.
- [53] Sam T Roweis and Lawrence K Saul. Nonlinear dimensionality reduction by locally linear embedding. *Science*, 290(5500):2323–2326, 2000.
- [54] Ron Rubinstein, Alfred M Bruckstein, and Michael Elad. Dictionaries for sparse representation modeling. *Proceedings of the IEEE*, 98(6):1045–1057, 2010.
- [55] Lawrence K. Saul and Sam T. Roweis. Think globally, fit locally: unsupervised learning of low dimensional manifolds. *Journal of Machine Learning Research*, 4(2):119–155, 2003.
- [56] Lawrence K Saul, Kilian Q Weinberger, Jihun H Ham, Fei Sha, and Daniel D Lee. Spectral methods for dimensionality reduction. *Semisupervised Learning*, pages 293–308, 2006.
- [57] Bernhard Schölkopf, Alexander Smola, and Klaus-Robert Müller. Nonlinear component analysis as a kernel eigenvalue problem. *Neural Computation*, 10(5):1299–1319, 1998.
- [58] John Shawe-Taylor and Nello Cristianini. *Kernel methods for pattern analysis*. Cambridge university press, 2004.
- [59] Jianbo Shi and Jitendra Malik. Normalized cuts and image segmentation. *IEEE Transactions on Pattern Analysis and Machine Intelligence*, 22(8):888–905, 2000.
- [60] Vin De Silva and Joshua B. Tenenbaum. Global versus local methods in nonlinear dimensionality reduction. In *Advances in Neural Information Processing Systems*, volume 15, pages 1959 – 1966, 2003.
- [61] Daniel A. Spielman, Huan Wang, and John Wright. Exact recovery of sparsely-used dictionaries. In *Conference on Learning Theory*, volume 23, 2012.
- [62] Joshua B Tenenbaum, Vin De Silva, and John C Langford. A global geometric framework for nonlinear dimensionality reduction. *Science*, 290(5500):2319–2323, 2000.
- [63] René Vidal. Subspace clustering. *IEEE Signal Processing Magazine*, 28(2):52–68, 2011.
- [64] Ulrike Von Luxburg. A tutorial on spectral clustering. *Statistics and Computing*, 17(4):395–416, 2007.
- [65] Fei Wang, Changshui Zhang, and Tao Li. Clustering with local and global regularization. *IEEE Transactions on Knowledge and Data Engineering*, 21(12):1665–1678, 2009.

- [66] Christopher K. I. Williams and Matthias Seeger. Using the nystrom method to speed up kernel machines. *Advances in Neural Information Processing Systems*, 13, 2001.
- [67] Christopher KI Williams. On a connection between kernel PCA and metric multidimensional scaling. *Machine Learning*, 46(1-3):11–19, 2002.
- [68] John Wright, Yi Ma, Julien Mairal, Guillermo Sapiro, Thomas S Huang, and Shuicheng Yan. Sparse representation for computer vision and pattern recognition. *Proceedings of the IEEE*, 98(6):1031–1044, 2010.
- [69] John Wright, Allen Y Yang, Arvind Ganesh, S Shankar Sastry, and Yi Ma. Robust face recognition via sparse representation. *IEEE Transactions on Pattern Analysis and Machine Intelligence*, 31(2):210–227, 2009.
- [70] Shuicheng Yan, Dong Xu, Benyu Zhang, Hong Jiang Zhang, Qiang Yang, and Stephen Lin. Graph embedding and extensions: A general framework for dimensionality reduction. *IEEE Transactions on Pattern Analysis and Machine Intelligence*, 29(1):40–51, 2007.
- [71] Jianchao Yang, Kai Yu, Yihong Gong, and Thomas Huang. Linear spatial pyramid matching using sparse coding for image classification. In *IEEE Conference on Computer Vision and Pattern Recognition*, pages 1794–1801. IEEE, 2009.
- [72] Zhirong Yang, Tele Hao, Onur Dikmen, Xi Chen, and Erkki Oja. Clustering by nonnegative matrix factorization using graph random walk. In *Advances in Neural Information Processing Systems*, pages 1088–1096, 2012.
- [73] Stella X Yu and Jianbo Shi. Multiclass spectral clustering. In *IEEE International Conference on Computer Vision*, pages 313–319. IEEE, 2003.
- [74] Ron Zass and Amnon Shashua. A unifying approach to hard and probabilistic clustering. In *IEEE International Conference on Computer Vision*, volume 1, pages 294–301. IEEE, 2005.
- [75] Lihi Zelnik-Manor and Pietro Perona. Self-tuning spectral clustering. In *Advances in Neural Information Processing Systems*, pages 1601–1608, 2004.